



## Pre-historic (

A. Morandi, Andrea Di Muro, C. Principe, G. Leroi, Laurent Michon, Patrick  
Bachèlery

### ► To cite this version:

| A. Morandi, Andrea Di Muro, C. Principe, G. Leroi, Laurent Michon, et al.. Pre-historic (

**HAL Id: hal-01147342**

**<https://hal.science/hal-01147342>**

Submitted on 27 Oct 2016

**HAL** is a multi-disciplinary open access archive for the deposit and dissemination of scientific research documents, whether they are published or not. The documents may come from teaching and research institutions in France or abroad, or from public or private research centers.

L'archive ouverte pluridisciplinaire **HAL**, est destinée au dépôt et à la diffusion de documents scientifiques de niveau recherche, publiés ou non, émanant des établissements d'enseignement et de recherche français ou étrangers, des laboratoires publics ou privés.

# Pre-historic (<5 kiloyear) Explosive Activity at Piton de la Fournaise Volcano

Andrea Morandi, Andrea Di Muro, Claudia Principe,  
Laurent Michon, Gabrielle Leroi, Francesco Norelli  
and Patrick Bachèlery

## Abstract

The characterization of the recent (<5 kiloyears) explosive activity and the research of violent paroxystic events over Piton de la Fournaise edifice has been performed through a drilling and excavation campaign supported by the integration of new radiocarbon ages to previous chronologic data. Fine grained “Bellecombe” phreatomagmatic ashes represent the product of the most violent explosive Piton de la Fournaise activity inside the investigated period. This activity results from a series of eruptions occurred over a time span much longer than previously thought. Anyhow, it represents the most traceable horizon (up to 13 km W-NW from the central cone) among the studied deposits and no other pyroclastic blanket exhibits a similar regional dispersion. The lack of a continuous lapilli/ash horizon from the proximal to

A. Morandi  
Department of Earth Sciences,  
University of Florence, Florence, Italy

A. Di Muro · G. Leroi  
Institut de Physique du Globe OVPF, Université  
Paris Diderot, Sorbonne Paris Cité, CNRS  
UMR-7154, 75005 Paris, France

C. Principe (✉) · F. Norelli  
Istituto di Geoscienze e Georisorse—CNR,  
via G. Moruzzi 1, 56124 Pisa, Italy  
e-mail: c.principe@igg.cnr.it

L. Michon  
Laboratoire Géosciences Réunion Université de La  
Réunion, Institut de Physique du Globe de Paris,  
Sorbonne Paris Cité CNRS, 97744 Saint-Denis,  
France

P. Bachèlery  
Laboratoire Magmas et Volcans UMR, Observatoire  
de Physique du Globe de Clermont-Ferrand.  
Université Blaise Pascal, CNRS-IRD 6524 5,  
rue Kessler, 63038 Clermont-Ferrand, France

distal areas points out that the lapilli cover on the volcano flank result of several local blankets linked to as many Hawaiian to Strombolian emission centers. As highlighted by new radiocarbon ages this kind of activity persisted along the N120 rift zone up to very recent times and ended probably just before the island's colonization, leaving no trace in historical records. The maximum expected magmatic event (Chisny-type eruption) has therefore to be related to intense Hawaiian fountaining. Its dangerousness is restricted to a relatively brief distance from the source and a regional deposition is strongly unlikely. The hazard represented by this type of activity resides in the possible positioning of the vent close to inhabited areas and in the possible occurrence of repeated events with short but unpredictable time interval from one to the other. Forecasting the location of the future eccentric eruptions is thus of paramount importance to minimize the potential impact of mild explosive eruptions on the inhabitants and the infrastructures.

## 1 Introduction

Piton de la Fournaise (PdF) is one of the most active basaltic intra-plate volcanoes. Even if the number of identified eruptive events depends on the completeness of written records (Lénat 2016, Chap. 1), at least 238 eruptions have been recognized since the second half of the 17th century, when permanent settlement on the island began (Ludden 1977; Bachèlery 1981; Lénat and Bachèlery 1988; Stieltjes and Moutou 1989; Roult et al. 2012; Di Muro et al. 2012; Michon et al. 2013). Since the establishment of permanent monitoring networks, coinciding with the foundation of Piton de la Fournaise Observatory (OVPF/IPGP) in 1979, there have been 61 instrumentally recorded eruptions. During the last 100 year, the average eruptive rate has been of about 1 eruption every 10 months and the longest eruptive pauses have occurred in recent times (1966–1972; 1992–1998) and have lasted up to 6 years. During recorded history, most of the eruptive vents were located close to the PdF central cone and more generally inside the horseshoe-shaped Enclos Fouqué depression, which encloses it. Only rare lateral eruptive fissures opened outside the Enclos Fouqué, along the NE and SE rift zones (Michon et al. 2016, Chap. 7; Staudacher et al. 2016, Chap. 9). Since human settlement on the island on 1638 CE, eruptive events have not been recorded along the

third and largest NW rift zone materialized by a N 120° trending cone alignment. However, the first settlements on La Réunion were located on the opposite coast of the island (NW coast) in respect to PdF. The corollary is that written records cover only a very short period at La Réunion, reliable written reports on PdF activity dating only back to 1754 CE (Michon et al. 2013). Therefore, it is of paramount importance to assess volcanic hazard over a period long enough to be representative of the variability in eruptive dynamics of PdF.

Nowadays, the island accounts for more than 830,000 permanent residents and ca. 470,000 tourists per year. Densely populated cities and villages are widespread on the whole active volcanic massif and progressively develop towards the most active volcanic zone. In recent times, effusive eruptions have periodically affected important infrastructure like the eastern national road, buildings and farmlands. In 1977 and 1986, the volcanic activity produced the opening of lateral eruptive fissures emitting lava that flowed through inhabited areas (Piton Sainte-Rose and Tremblet, respectively) up to the sea-shore (Delorme et al. 1989; Kieffer et al. 1977).

Recent review of historic reports has revealed that weak to mild phreatic and phreatomagmatic ash plumes (the most violent corresponding to the 1860 CE eruption) repeatedly punctuated the dominantly effusive activity of the central cone, spreading fine ash on the volcano edifice and

sometimes over most of La Réunion Island (Bachèlery 1981; Villeneuve and Bachèlery 2006; Peltier et al. 2012; Michon et al. 2013). Dispersal of Pele's hairs over the whole island can also occur, as in 1939 and in 2007 (Michon et al. 2013). More violent explosive phreatic to phreatomagmatic eruptions of PdF have traditionally been related to major old caldera forming events contributing to the formation of the Enclos Fouqué caldera. The Bellecombe Ash unit would account for such paroxysmal events around 4175–3200 BP (Bachèlery 1981; Mohamed-Abchir 1996). This chapter reviews the dynamics of pre-historic eruptions of PdF, whose age is comprised between the Bellecombe Ash unit and the recorded history. Magmatic explosive activity, like violent strombolian or subplinian events, cannot be a priori discarded even for a basaltic volcano in an intraplate environment. Even if effusive or mild explosive dynamics of Strombolian and Hawaiian types characterize the basaltic volcanic activity, it has been since long recognized that mafic magmas can produce violent explosive events, with ash columns up to 30 km high and their products spreading over an area of tens to more than 1000 km<sup>2</sup> (MacDonald 1972; Arrighi et al. 2001; Houghton et al. 2004; Sable et al. 2006, 2009; Pioli et al. 2008; Andronico et al. 2009; Wong and Larsen 2010). The possible occurrence of such kind of events has thus motivated the recent re-assessment of volcanic hazard at La Réunion (Di Muro et al. 2012). In this chapter, we address this issue by integrating previous and new stratigraphic and chronologic data obtained on stratigraphic sections and shallow drillings (<10 m).

---

## **2 Wind Distribution Over La Réunion Island and Microstratigraphic Drilling Strategy**

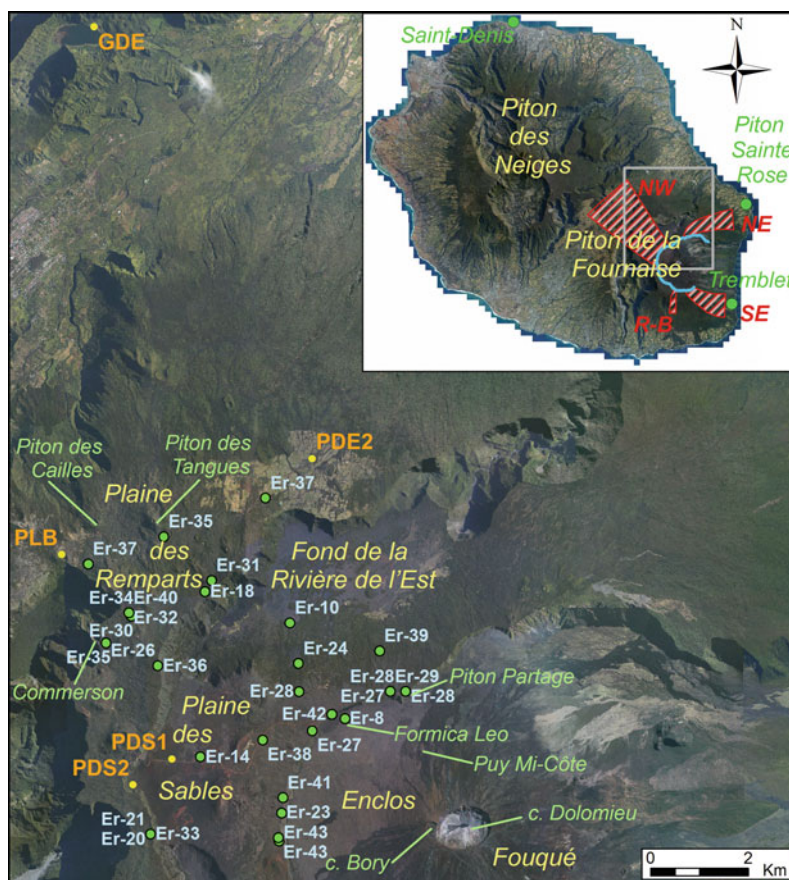
Wind direction and strength play an important role on the regional distribution of pyroclastic products dispersed by vertical plumes carrying ash and lapilli. This is particularly true for the

finest particles that can be carried tens to hundreds of kilometers away from the eruptive source. The main synoptic winds over La Réunion Island are the Trade winds that blow northwestwards dominating the air circulation at ground level (Trenberth et al. 1990). Local breezes effects become more influent mostly in downwind and protected areas, where the surface winds are weaker (Lesouëf et al. 2011).

The vertical winds distribution over La Réunion shows a marked inversion of their direction at an altitude of about 3000–4000 m asl (Taupin et al. 1999), depending on the season. The dispersion of pyroclasts is therefore strongly controlled by the height of the eruptive column. Examples are given by the ash and aerosol plumes generated during the April 2007 eruption, when an initial westward spreading of small ash and gas plumes was followed by a clockwise rotation toward N and NE sectors as the aerosol plume exceeded 4 km height (Tulet and Villeneuve 2011). Ash dispersal during recent phreatomagmatic explosive eruptions (e.g. 1860 CE) confirms this trend and suggests even the possibility of a splitting of the eruptive columns (Hugoulin 1860; Villeneuve and Bachèlery 2006). In agreement with this winds pattern, only sparse low amounts of basaltic shards, possibly attributed to PdF explosive events, were identified during the last 30 k year in a deep-sea marine core located south of the volcano edifice (Fretzdorff et al. 2000; Sisavath et al. 2012). Consequently, we performed in 2011 new microstratigraphic drillings and surface outcrops descriptions along a N-NW axis, between the proximal area (Plaine des Sables, about 5 km from the central cone) and the distal area (Grand Étang, 18 km NW from the summit vents), passing through the N120 rift zone. As a whole, 30 outcrops were described and 5 drillings were performed (Fig. 8.1).

The investigation of the spatial distribution of pyroclastic deposits must take carefully into account their potential preservation over the territory. This is particularly true in the tropical environment of La Réunion where a steep, pronounced topography is associated with extreme weather conditions (up to 6 m of rain per year

**Fig. 8.1** Drilling locations (yellow dots) and dated eruptive events, inside stratigraphic sections, younger than 5000 year (green dots) on the NW rift. In the upper right corner: the Enclos Fouqué rim (light blue) and the three major rift zones (red areas) intersecting the PdF massif are shown. NW, SE and NE stand respectively for NW, SE and NE rift; R-B is the Ramond-Baril eruptive axis, corresponding to a N-S scoria cones alignment



and wind speed up to 250 km/h; Météo France source). Such a natural background produces a high rate of removal and reworking especially on the incoherent and easy-erodible pyroclastic sediments. The preservation potential of loose lapilli fallouts or thin ash layers (typical of small eruptions or distal outcrops) is therefore very low. As an example, the 1–2 cm-thick ash deposit from the 1986 Dolomieu phreatic explosion on the slopes of the summit cone of PdF was completely removed in less than one week, after two rainy days. In order to overcome these severe constraints, we selected low-energy sedimentation environments as drilling sites. This condition is better achieved in the endorheic volcanic lakes where the sedimentation is a quite sporadic event (Principe et al. 1997, 2007). In these setting, the deposition of tephra is limited to primary fallout deposits and the reworking is restricted to the bank's material. At La Réunion,

this kind of sampling point is represented by intracrateric ponds on the top of strombolian cones spotted over the territory. On the other hand, we have to stress that the volume of these permanent ponds/lakes is highly sensitive to the alternation of extreme pluviometric conditions and dryer periods. In other terms the sedimentation conditions are never optimal. To reach the selected locations, we used a portable drilling system (AF topcore 40 modified; Fig. 8.2a, b), able to produce 10 m long continuous and undisturbed micro-cores (Principe et al. 1997). This method is able to avoid the loss of information even for very thin layers, due to the presence of a textile sheet around the core (Fig. 8.2c). Wherever possible, the condensed tephra sequences, which sediment on the lakes shores, are drilled in order to reach the maximum length of tephra record with the minimum coring depth (Principe et al. 2007).



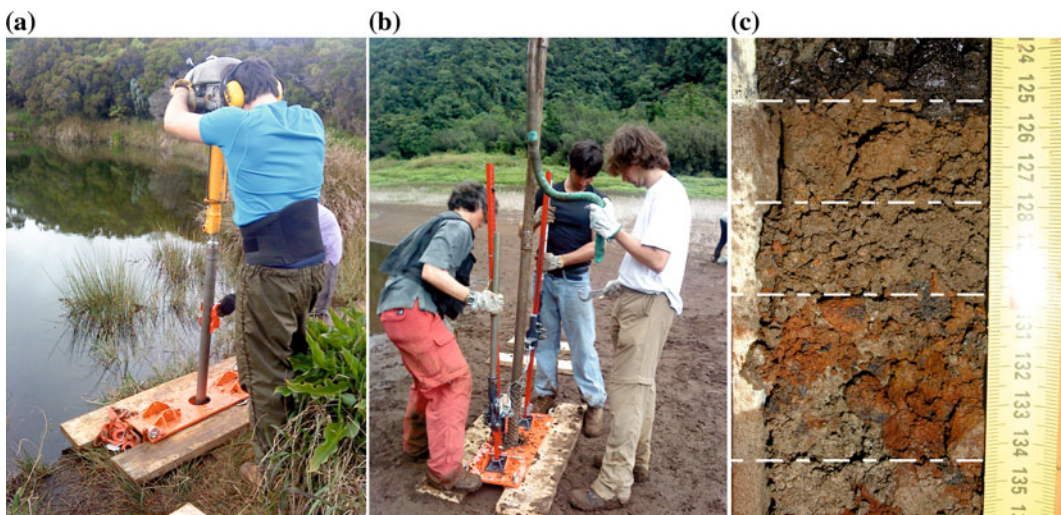


**Fig. 8.2** AF topcore 40 modified coring system and drilling operation. **a** The infission is performed by a jackhammer thrust, while **b** the extraction by a mechanical jack system. **c** Thin ash beds preserved in the PDS2 core

### 3 Drilled Cores and Outcrop Description

The performed cores have been opened in laboratory for description and sampling (Fig. 8.2c). Macroscopical description has been performed and tephra layers have been characterized by means of their color, texture, granulometry, componentry and mineralogical assemblage. Thanks to the broad spreading of the grey, fine-grained Bellecombe Ash falls and to their peculiar mineral assemblage, i.e. abundant pyroxene + olivine crystals together with gabbro fragments and rare quartz crystals, they represented a perfect stratigraphic marker to identify tephra sequences younger than ca. 4000 year in the proximal-medial areas of the volcano.

In the Grand Étang distal drilling (GDE; Table 8.2) two units of fine ashes overlie the proximal facies of a scoria cone, they contain a variable amount of granule to pebble-size clasts, the lower unit is characterized by the presence of organic matter. In the middle sector, Piton de l'Eau core (PDE2; Table 8.3) shows, within the scoria cone edifice (represented by the lower poorly sorted breccia), the presence of fine-grained deposits related to a reddish ashy

paleosol containing organic matter and an upper stratigraphic succession of ashes which includes the Bellecombe Ash unit. Piton dans le Bout core (PLB; Table 8.4) is instead made of six units, of approximately alternating lapilli and ash beds. Bellecombe Ash unit underlies the uppermost black lapilli bed. We here stress that the “Bellecombe ash unit” group a sequence of events spanning about 2 millennia. The cpx-gabbro rich “Bellecombe ashes” cropping out in the Piton de l'eau—Piton dans le Bout area has been dated at  $3735 \pm 90$  and  $3715 \pm 30$  BP (Table 8.1). Younger ages in the range  $3110 \pm 30$  BP– $3060 \pm 35$  have been obtained for the uppermost beds of the “Bellecombe ash unit” along the Langevin plateau (Table 8.1). Notably, the ages of the lowermost beds in the “Bellecombe unit” cropping out in the proximal-medial area are somewhat older ( $4880 \pm 35$  BP;  $4175 \pm 145$  BP; Table 8.1) than the uppermost beds, which attain the medial and distal sectors.

In the proximal sector, the two cores of the Plaine des Sables (PDS2 and PDS1; Tables 8.5 and 8.6) show, above the Bellecombe Ash unit, the presence of a black, glassy, and largely reworked lapilli sequence, which is intercalated with thin lava flows when approaching the Piton Chisny cone. In Tables 8.2, 8.3, 8.4, 8.5 and 8.6

**Table 8.1** Dated eruptive event at Piton de La Fournaise volcano

Eruption ID	Location	Unit name	Unit type	Note on the sample	Coordinates		Dating method	Age (BP)	±	Median probability (A.D.)	Calibrated min (A.D.) 2σ	Calibrated max (A.D.) 2σ
					x	y						
Er-1	RZNE	1998 lava flow	Lava flow							1998	1998	1998
Er-2	RZSE	1986 lava flow	Lava flow							1986	1986	1986
Er-3	RZNE	1977 lava flow	Lava flow							1977	1977	1977
REU140212-10/9	Central activity	Partage cliff	Ash beds	Historical eruptions; B layer; multiple fragments	366,212.7	7,653,718.8	14C	120	30	1831	1939	1679
REU140212-S1-2b	Central activity	Partage cliff	Ash beds	Historical eruptions; B1 layer; top of historical sequence; single fragment	365,582.4	7,653,224.7	14C	130	30	1821	1941	1675
Er-4	RZSE	1800 lava flow	Lava flow							1802	1802	1802
Er-10	N120	Piton Rampe 14	Strombolian cone	Below the lava flow	363,034.827	7,654,507.466	14C	140	90	1791	nd	1528
AND 02 / REU140721 / S1	N120	Trous Blancs area	Modern soil	Uppermost layer rich in roots and organic matter; multiple fragments	355,338.72	7,655,654.69	14C	145	30	1801	1948	1668
REU031014-3	N120	Rivière des Remparts					14C	150	30	1785	1950 (nd)	1667
Er-5	RZSE	1776 lava flow	Lava flow							1776	1776	1776
Er-6	RZSE	1774 lava flow	Lava flow							1776	1774	1774
REU140212-S4-2	Central activity	Partage cliff	Ash beds	Historical eruptions; B layer; top of historical sequence; multiple fragments	364,086.9	7,653,098.6	14C	160	30	1773	1950 (nd)	1664
REU140521-BB1	RZNE	Piton Moka (near Anses des Cascades)	Ash beds	In lapilli fall above the lahar reworking Bellecombe breccia; modern agricultural activity? multiple fragments	376,943.4	7,656,622.4	14C	175	30	1770	1950 (nd)	1657
AND 08 / REU140728-2a / S1	N120	Top of Trous Blancs site	Modern soil		355,672.20	7,654,589.84	14C	195	30	1770	1950 (nd)	1648
Er-7	RZSE	Puy Raymond	Strombolian cone	Inside ashes. 1 m below the lava flow	365,883.571	7,645,619.532	14C	45-115	75		nd	nd

(continued)

**Table 8.1** (continued)

Eruption ID	Location	Unit name	Unit type	Note on the sample	Coordinates		Dating method	Age (BP)	±	Median probability (A.D.)	Calibrated min (A.D.) 2σ	Calibrated max (A.D.) 2σ
					x	y						
Er-8	EF (lava above the Formica leo cone)	CLEF lava field	Lava field	Pahoehoe lava	364,160.653	7,652,535.955	Archeomagnetic			1750	ca. 1750	
Er-8	EF	CLEF lava field	Lava field	Pahoehoe lava			Historical sources			1740	1730	1750
Er-9	RZNE	1708 lava flow	Lava flow							1708	1708	1708
Er-8	EF (lava close to Bellecombe steps)	CLEF lava field	Lava field	Sample RE-90-28; pahoehoe	364,160.653	7,652,535.955	Cosmogenic	250	800	1700	nd	nd
REU140212-S1-2a	Central activity	Partage cliff	Ash beds	Historical eruptions; B1 layer; top of historical sequence; multiple fragments	365,582.4	7,653,224.7	14C	255	30	1650	1950 (nd)	1521
Er-11	RZNE	Piton Nelson—Piton de Bois Blancs	Strombolian cone	Near Bois Blanc village	374,006.015	7,654,760.755	14C	260	80	1643	nd	1450
REU140320-S5-4	Central activity	Partage cliff	Ash beds	Historical eruptions; multiple fragments	366,109.7	7,653,616.5	14C	340	30	1559	1639	1470
Er-12	RZSE	Piton Taipoul	Strombolian cone	Below the scoriae of the cone and above an ash bed	366,430.576	7,645,458.601	14C	355	75	1549	1794	1427
Er-13	RZSE	Mare Longue lava flow	Lava flow	Below the lava flow			14C	364	25	1517	1632	1451
Er-15	N120	Piton Chisny—lava with dunite enclaves near Chisny cone	Polyphase cone	Near Chisny cone; phase 2 in Bachelery <a href="#">1981</a>			Archeomagnetic			1500	1600	1400
Er-16	RZNE	Piton Indivis - Bois Blanc	Strombolian cone		376,033.1	7,655,634.376	14C	420	80	1500	1649	1327
Er-14	N120	Piton Chisny—Plaine des Sables black scoria fall	Multiple cones	Section 20; Plaine des Sables. near Piton Chisny	361,198.937	7,651,746.67	14C	381	26	1493	1630	1445
Er-17	RZSE	Ravine d'Ango lava	Strombolian cone	In conglomerate below the lava (the soil is not burned)	374,511.652	7,638,425.555	14C	455	70	1457	1635	1318
Er-18	N120	Petit Cratère	Strombolian cone	Below the lava flow	361,293.907	7,655,150.227	14C	470	75	1443	1634	1305
Er-19	RZSE	Le Baril 1 (Brulé du Baril)	Strombolian cone	Basal scoriae below the lava flow (Ravine	365,841.284	7,638,409.566	14C	575	75	1358	1444	1281

(continued)



**Table 8.1** (continued)

Eruption ID	Location	Unit name	Unit type	Note on the sample	Coordinates		Dating method	Age (BP)	±	Median probability (A.D.)	Calibrated min (A.D.) 2σ	Calibrated max (A.D.) 2σ
					x	y						
				Perote river) and above a soil								
Er-20	N120	Langevin plateau fall—bed 4	Scoriae bed	Section 1—Caldera des Sables cliff	360,176.998	7,650,157.619	14C	620	30	1349	1399	1292
Er-21	N120	Langevin plateau fall—bed 5	Scoriae bed	Section 1—Caldera des Sables cliff	360,176.998	7,650,157.619	14C	868	30	1177	1251	1046
Er-22	N120	“Piton Chisny lavas” in Langevin valley	Lava flow	Below aa lava flow in the Langevin valley	359,323.842	7,640,947.249	14C	1105	60	925	1022	775
Er-24	N120	Piton sous le Gite	Strombolian cone	Below the lava flow	363,211.109	7,653,672.45	14C	1465	75	578	675	420
Er-23	Central activity?	Ashes on western rim of Enclos Fouqué (near Chisny)	Ash beds		362,860.285	7,650,591.453	14C	1450	250	576	1122	50
Er-25	N120	Tephra on Les Troux Blancs	Scoria bed	Sample REU 1301-243 Trou Blanc	356,229.000	7,654,133.000	14C	1495	30	573	641	434
Er-26	N120	Commerson crater	Scoria bed		359,258.678	7,654,094.665	14C	1890	55	119	249	−20
Er-27	Central activity	Partage Tephra (Unit 3; CC2 layer)	Scoria bed	Section 6 (Partage cliff)	365,088.054	7,653,096.733	14C	2140	35	−179	−52	−356
Er-27	Central activity	Ashes on NW cliff of Enclos Fouqué (Bellecombe cliff)	Ash bed	Ashes draping the lower third of the Enclos Fouqué cliff	363495.684	7652284.643	14C	2140	80	−184	1	−381
Er-28	Central activity	Ashes near the “Gite du Volcan” (“Cendres de Bellecombe” in B’81 and V&B’82)	Ash beds	Sampled near the Gites du Volcan	363,223.126	7,653,091.586	14C	2320	90	−403	−178	−755
Er-28	Central activity	Partage Tephra (Unit 2; CC1 layer)	Ash bed	Section 6 (Partage cliff)	365,088.054	7,653,096.733	14C	2340	30	−402	−366	−506
Er-28	Central activity	Ashes near the “Gite du Volcan”	Ash beds	Upper part of an ash bed. below a bed of scoriae	365,412.448	7,653,098.027	14C	2390	85	−521	−235	−784
Er-28?	N120	Piton des Tangués tephra (Below Red Tephra Unit)	Lapilli bed?	Ash or lapilli bed above the Upper Bellecombe ash			14C	2665	615	−841	608	−2345
Er-29	Central activity	Partage Tephra (Unit1; CC0 layer)	Ash bed	Section 6 (Partage cliff)	365,088.054	7,653,096.733	14C	2855	35	−1021	−919	−1121
REU140825-PDT2	N120	Near Piton des Tangués parking	Ash beds	Black soil below red tephra lapillis covering Bellecombe falls	360,408.8	7,656,179.8	14C	2920	30	−1115	−1020	−1211

(continued)

**Table 8.1** (continued)

Eruption ID	Location	Unit name	Unit type	Note on the sample	Coordinates		Dating method	Age (BP)	±	Median probability (A.D.)	Calibrated min (A.D.) 2σ	Calibrated max (A.D.) 2σ
					x	y						
Er-30	Central activity	Upper unit of Bellecombe ash	Ash bed	Sample REU 1303-07 A1	359,775.000	7,654,645.000	14C	3060	35	−1326	−1228	−1411
Er-31	N120	Piton Sauvetage	Strombolian cone	Ash bed	361,424.89	7,655,382.022	14C	3085	75	−1335	−1127	−1501
Er-32	Central activity	Upper unit of Bellecombe ash	Ash bed	Sample REU 1303-07 A2 2A	359,728.000	7,654,714.000	14C	3095	30	−1350	−1280	−1428
Er-33	N120	Langevin plateau fall- bed 6	Ash and lapilli bed	Section 1—Caldera des Sables cliff	360,176.998	7,650,157.619	14C	3100	30	−1355	−1284	−1431
Er-34	Central activity	Upper unit of Bellecombe ash	Ash bed	Sample REU 1303-07 A2 2C/1 km west of Piton des Basaltes	359,728.000	7,654,714.000	14C	3110	30	−1377	−1288	−1437
Er-41	Central activity	Lava3 of W Enclos Fouqué rim	Lava flow	Sample RE-90-15b (below Bellecombe ash); oceanite	362,889.735	7,650,907.916	Cosmogenic	3340	1012	−1390		
REU140822-2	N120	0.5 km from Nez de Bœuf, above Bellecombe ash fall	Ash beds	Soil above Bellecombe and below a thin lapilli layer	357,317	7,655,847	14C	3130	30	−1407	−1300	−1494
Er-41	Central activity	Lava3 of W Enclos Fouqué rim	Lava flow	Sample RE-90-15a (below Bellecombe ash); oceanite	362,889.735	7,650,907.916	Cosmogenic	3420	820	−1470		
Er-35	N120	Piton des Tangués ashes ; Upper Bellecombe ash (U3a)?	Ash bed	Cpx-gabbro rich ash bed (above Piton des Tangués cone; Below Red Tephra Unit)	360,442.092	7,656,281.636	14C	3205	75	−1483	−1288	−1656
Er-35	N120	Ashes near commerson (below red tephra unit)	Ash bed	Fine ash bed near commerson	359,258.678	7,654,094.665	14C	3220	50	−1495	−1411	−1615
Er-42	Central activity	Lava2 of NW Enclos Fouqué rim	Lava flow	Sample RE-90-31 (below partage unit)	363,890.37	7,652,624.595	Cosmogenic	3500	1150	−1550		
Er-36	N120	Piton des Basaltes	Strombolian cone	Scoriae bed	360,326.603	7,653,622.523	14C	3305	55	−1584	−1453	−1735
Er-37	Central activity	Bellecombe ash; upper bellecombe ash (U3a?)	Ash bed	Sample REU 1303-07 A6/About 1 km east of Piton dans l'bout	358,895.000	7,655,721.000	14C	3715	30	−2098	−2029	−2200

(continued)

**Table 8.1** (continued)

Eruption ID	Location	Unit name	Unit type	Note on the sample	Coordinates		Dating method	Age (BP)	±	Median probability (A.D.)	Calibrated min (A.D.) 2σ	Calibrated max (A.D.) 2σ
					x	y						
Er-37	Central activity	Piton des Tangués ashes; upper Bellecombe ash (U3a)?	Ash beds	Cpx-gabbro rich ash bed (above Piton des Tangués lava; below red Tephra unit)	362,534.552	7,657,077.969	14C	3735	90	−2148	−1920	−2456
Er-43	Central activity	Lava1 of W Enclos Fouqué rim	Lava flow	Sample RE-90-24a	362,798.548	7,650,082.1	Cosmogenic	4310	821	−2360		
Er-43	Central activity	Lava1 of W Enclos Fouqué rim	Lava flow	Sample RE-90-25	362,806.183	7,650,013.384	Cosmogenic	4550	1270	−2600		
AND 02/ REU140721/ S3b	N120	Trous Blanc site (S3b ash below Bellecombe and above Trous Blanc eruption)	Ash beds	Charcoals at the base of S3B yellow layer (unit just below Bellecombe fall)	355,338.72	7,655,654.69	14C	4115	30	−2693	−2577	−2865
Er-38	Central activity	Lower Bellecombe ash Unit (U1b)	Ash beds	Fossil wood (unburned)	362,477.784	7,652,096.79	14C	4175	145	−2746	−2307	−3316
AND 04/ REU140723-1/ S3b	N120	Piton Sec (S3b ash below Bellecombe)	Ash beds	Charcoals at the base of S3B yellow layer (unit just below Bellecombe fall)	355,201.53	7,655,305.20	14C	4400	30	−3013	−2917	−3261
AND 08/ REU140728-2a/ bglaBR	N120	Trous Blancs site; top of the Trous Blancs Breccia	Ash beds	Charcoals at the base of L2(?) orange red layer (unit just below Bellecombe fall)	355,672.20	7,654,589.84	14C	4685	30	−3447	−3370	−3625
AND 12/ REU140801-2	N120	At the feet of Nez de Bœuf spatter (below Bellecombe)	Ash beds	Soi below thin lapilli; layer just below Bellecombe fall	356,562.22	7,654,352.30	14C	4695	35	−3454	−3370	−3629
Er-39	Central activity	Lava2 of NW Enclos Fouqué rim	Lava flow	Basal scoriae below the uppermost lava flow near Bellecombe (below Partage unit)	364,873.000	7,653,932.000	14C	4745	130	−3515	−3100	−3794
Er-40	Central activity	Second unit of Bellecombe ash	Ash bed	Sample REU 1303-07 A2 2b/1 km west of Piton des Basaltes	359,728.000	7,654,714.000	14C	4880	35	−3669	−3540	−3758
Er-43	Central activity	Lava1 of W Enclos Fouqué rim	Lava flow	Sample RE-90-24b; oceanite	362,798.548	7,650,082.1	Cosmogenic	5130	690	−3180		
AND 02/ REU140721/ S3a	N120	Trous Blancs area	Ash beds	S3a ashes above the Trous Blanc eruption	355338.72	7655654.69	14C	5400	35	−4277	−4077	−4341

(continued)

**Table 8.1** (continued)

Eruption ID	Location	Unit name	Unit type	Note on the sample	Coordinates		Dating method	Age (BP)	±	Median probability (A.D.)	Calibrated min (A.D.) 2σ	Calibrated max (A.D.) 2σ
					x	y						
REU140825-PDT1	N120	Piton des Tangués parking	Ash beds	Thick red lahar below Bellecombe falls	360,408.8	7,656,179.8	14C	5570	35	−4406	−4346	−4460
Er-44	Piton des Neiges?	Grand Etang deep drilling	Conglomerate	Fossil wood (unburned) in conglomerates at the base of the Puy de l'Etang ashes	359,436.931	7,666,718.692	14C	5730	110	−4584	−4352	−4823
Er-45	N120	“Les Trous Blancs” lava field	Lava flow		356,050.106	7,654,462.838	Stratigraphic	6500				
Er-46	N120	Ashes along the path to “Piton des Tangués”	Ash beds	Section 12; layer 5 (above the “Cendres de Notre Dame” unit)	360,408.937	7,656,181.043	14C	6965	38	−5847	−5745	−5975
Er-47	N120	Piton textor	Ash beds		358,199.373	7,656,293.751	14C	7125	125	−5999	−5740	−6231
Er-48	N120	Ashes between Piton textor and Piton des Cailles	Ash beds		358,729.735	7,656,540.14	14C	7930	90	−6837	−6611	−7060
AND 04/ REU140723-1/ S3a	N120	Trous Blancs area (near Piton sec; above Trous Blancs eruption)	Ash beds	S3a ash layer	355,201.53	7,655,305.20	14C	7985	40	−6915	−6709	−7051
Er-49	N120	Piton dans le bout	Strombolian cone		358,474.994	7,655,901.2	14C	9355	190	−8658	−8254	−9223
AND 06/ REU140723-3/ S3b	N120	Near Piton Sec (S3b ashes above the Trous Blanc eruption)	Ash beds		355,352.97	7,655,202.68	14C	9430	45	−8712	−8572	−8823
Er-50	Piton des la Fournaise?	Grand Etang deep drilling	Conglomerate	Fossil wood in conglomerate below the deep lavas (−40 m) met by the drill	359,436.931	7,666,718.692	14C	10,650	110	−10,644	−10,238	−10,801
REU031014-1BC	Piton des Neiges	Bras des Lianes					14C	12,040	60	−11,942	−11,802	−12,111
Er-51	Central activity	Notre Dame de la Paix -2	Ash beds		353,792.779	7,646,998.349	14C	15,200	1300	−16,378	−12,873	−19,716
LAS 17/ REU140718-1/ Part B	N120	Bois Court lava flow	Lava flow		348,715.72	7,655,411.65	14C	17,780	110	−19,582	−19,222	−19,908

(continued)

**Table 8.1** (continued)

Eruption ID	Location		Unit name	Unit type	Note on the sample	Coordinates		Dating method	Age (BP)	±	Median probability (A.D.)	Calibrated min (A.D) 2σ	Calibrated max (A.D.) 2σ	
						x	y							
LAS 17/ REU140718-1/ Part A	N120		Bois Court lava flow	Lava flow		348,715.72	7,655,411.65	14C	17,840	100	−19,664	−19,347	−19,948	
LAS 17/ REU140718-1/ Part C	N120		Bois Court lava flow	Lava flow		348,715.72	7,655,411.65	14C	17,970	100	−19,817	−19,507	−20,114	
Er-52	Central activity		“Cendres de Notre Dame” Unit	Ash beds				Stratigraphic	19,000–37,000					
Er-53	N120		Bois court	Strombolian cone	Altered ash layer, below the lava flow	348,644.795	7,655,086.233	14C	19,185	265	−21,168	−20,540	−21,776	
Er-54	Central activity		Plaine des Sables caldera fault	Caldera fault	Sample RE-90-07; surface of the caldera fault	360,074.551	7,650,976.811	Cosmogenic	23,800	2000	−21,850	−21,478	−30,115	
Er-55	N120		Piton Manuel—Piton des Cabris	Strombolian cone		351,186.326	7,653,685.743	K/Ar	29,000		−27,050			
Er-56	Central activity		Notre Dame de la Paix -1	Ash beds		354,230.713	7,647,126.81	14C	37,200	1500	−39,467	−36,591	−42,016	
Er-57	N120 SVZ		Piton Rouge (St. Joseph)	Strombolian cone		356,019.22	7,638,466.955	K/Ar	57,000		−55,050			
Er-58	Central activity		Summit lava of the Plaine des Ramparts	Lava flow	Sample RE-90-06; last lavas of the caldeira	359,640.634	7,651,410.728	Cosmogenic	62,000	4000	−60,050			
Er-59	Central activity?		Submarine tephra (S17-656 drill)	Ash bed	Sample R4-1; basaltic ash			18O	67,000	5000	−65,050			
Eruption ID	Location	Unit name	Unit type	Note on the sample	Calibrated probability distribution (A.D.)—Max probability 2σ			Calibrated probability distribution (A.D.)—Secondary probability 2σ			Calibrated probability distribution (A.D.)—Tertiary probability 2σ			Reference
					Min age	Max age	% prob.	Min age	Max age	% prob.	Min age	Max age	% prob.	
Er-1	RZNE	1998 lava flow	Lava flow											Michon et al. (2013)
Er-2	RZSE	1986 lava flow	Lava flow											Michon et al. (2013)
Er-3	RZNE	1977 lava flow	Lava flow											Michon et al. (2013)
REU140212-10/9	Central activity	Partage cliff	Ash beds	Historical eruptions; B layer; multiple fragments	1939	1801	65.9	1764	1679	34.1				This chapter
REU140212-S1-2b	Central activity	Partage cliff	Ash beds	Historical eruptions; B1 layer; top of historical sequence; single fragment	1894	1799	44.4	1777	1675	39.9	1941	1905	15.7	This chapter

(continued)

**Table 8.1** (continued)

Eruption ID	Location	Unit name	Unit type	Note on the sample	Calibrated probability distribution (A.D.)–Max probability 2σ			Calibrated probability distribution (A.D.) –Secondary probability 2σ			Calibrated probability distribution (A.D.)–Tertiary probability 2σ			Reference
					Min age	Max age	% prob.	Min age	Max age	% prob.	Min age	Max age	% prob.	
Er-4	RZSE	1800 lava flow	Lava flow											Michon et al. (2013)
Er-10	N120	Piton Rampe 14	Strombolian cone	Below the lava flow										–
AND 02 / REU140721 / S1	N120	Trous Blancs area	Modern soil	Uppermost layer rich in roots and organic matter; multiple fragments	1890	1797	35	1781	1716	30.7	1711	1668	17.2	This chapter
REU031014-3	N120	Rivière des Remparts			1783	1717	33.2	1889	1831	19.5	nd	1910	18.1	This chapter
Er-5	RZSE	1776 lava flow	Lava flow											Michon et al. (2013)
Er-6	RZSE	1774 lava flow	Lava flow											Michon et al. (2013)
REU140212-S4-2	Central activity	Partage cliff	Ash beds	Historical eruptions; B layer; top of historical sequence; multiple fragments	1820	1719	50.1	nd	1913	18.4	1706	1664	17.8	This chapter
REU140521-BB1	RZNE	Piton Moka (near Anses des Cascades)	Ash beds	In lapilli fall above the lahar reworking Bellecombe breccia; modern agricultural activity? multiple fragments	1815	1725	55.6	1696	1657	19.4	nd	1917	18.7	This chapter
AND 08 / REU140728-2a / S1	N120	Top of Trous Blancs site	Modern soil		1811	1728	57.6	1691	1648	25.2	nd	1922	17.2	This chapter
Er-7	RZSE	Puy Raymond	Strombolian cone	Inside ashes. 1 m below the lava flow										–
Er-8	EF (lava above the Formica leo cone)	CLEF lava field	Lava field	Pahoehoe lava										Tanguy et al. (2011)
Er-8	EF	CLEF lava field	Lava field	Pahoehoe lava										Michon et al. (2013)
Er-9	RZNE	1708 lava flow	Lava flow											Michon et al. (2013)
Er-8	EF (lava close to Bellecombe steps)	CLEF lava field	Lava field	Sample RE-90-28; pahoehoe										–

(continued)



**Table 8.1** (continued)

Eruption ID	Location	Unit name	Unit type	Note on the sample	Calibrated probability distribution (A.D.)—Max probability $2\sigma$			Calibrated probability distribution (A.D.)—Secondary probability $2\sigma$			Calibrated probability distribution (A.D.)—Tertiary probability $2\sigma$			Reference
					Min age	Max age	% prob.	Min age	Max age	% prob.	Min age	Max age	% prob.	
REU140212-S1-2a	Central activity	Partage cliff	Ash beds	Historical eruptions; B1 layer; top of historical sequence; multiple fragments	1675	1621	59.1	1579	1521	21.3	1799	1777	16.4	This chapter
Er-11	RZNE	Piton Nelson—Piton de Bois Blancs	Strombolian cone	Near Bois Blanc village										Bachèlery (1981)
REU140320-S5-4	Central activity	Partage cliff	Ash beds	Historical eruptions; multiple fragments	1639	1470	100							This chapter
Er-12	RZSE	Piton Taipoul	Strombolian cone	Below the scoriae of the cone and above an ash bed										Tanguy et al. (2011)
Er-13	RZSE	Mare Longue lava flow	Lava flow	Below the lava flow										Straberg (comm pers)
Er-15	N120	Piton Chisny—lava with dunite enclaves near Chisny cone	Polyphase cone	Near Chisny cone; phase 2 in Bachèlery (1981)										Tanguy et al. (2011)
Er-16	RZNE	Piton Indivis—Bois Blanc	Strombolian cone											Bachèlery (1981), map, Tanguy et al. (2011)
Er-14	N120	Piton Chisny—Plaine des Sables black scoria fall	Multiple cones	Section 20; Plaine des Sables. near Piton Chisny										Di Muro et al. (2012)
Er-17	RZSE	Ravine d'Ango lava	Strombolian cone	In conglomerate below the lava (the soil is not burned)										Tanguy et al. (2011)
Er-18	N120	Petit Cratère	Strombolian cone	Below the lava flow	1529	1384	69.8	1634	1544	17	1364	1305	13.2	Tanguy et al. (2011)
Er-19	RZSE	Le Baril 1 (Brulé du Baril)	Strombolian cone	Basal scoriae below the lava flow (Ravine Perote river) and above a soil	1444	1281	100							Tanguy et al. (2011)
Er-20	N120	Langevin plateau fall—bed 4	Scoriae bed	Section 1—Caldera des Sables cliff	1399	1292	100							Di Muro et al. (2012)

(continued)

**Table 8.1** (continued)

Eruption ID	Location	Unit name	Unit type	Note on the sample	Calibrated probability distribution (A.D.)—Max probability $2\sigma$			Calibrated probability distribution (A.D.)—Secondary probability $2\sigma$			Calibrated probability distribution (A.D.)—Tertiary probability $2\sigma$			Reference
					Min age	Max age	% prob.	Min age	Max age	% prob.	Min age	Max age	% prob.	
Er-21	N120	Langevin plateau fall—bed 5	Scoriae bed	Section 1—Caldera des Sables cliff	1251	1148	79.5	1090	1046	16.1	1139	112	4.4	Di Muro et al. (2012)
Er-22	N120	“Piton Chisny lavas” in Langevin valley	Lava flow	Below aa lava flow in the Langevin valley	1022	775	100							Albarède et al. (1997), pg. 174, Tanguy et al. (2011)
Er-24	N120	Piton sous le Gite	Strombolian cone	Below the lava flow	675	420	100							–
Er-23	Central activity?	Ashes on western rim of Enclos Fouqué (near Chisny)	Ash beds		1047	50	98.9	1122	1088	0.7				Bachèlery (1981), pg. 137
Er-25	N120	Tephra on Les Troux Blancs	Scoria bed	Sample REU 1301-243 Trou Blanc	641	534	93.8	487	470	3.2	453	434	2.9	This chapter
Er-26	N120	Commerson crater	Scoria bed		249	–1	99.5	–12	–20	0.5				Bachèlery (1981), Tanguy et al. (2011)
Er-27	Central activity	Partage Tephra (Unit 3; CC2 layer)	Scoria bed	Section 6 (Partage cliff)	–54	–231	78.2	–292	–354	21.8				Di Muro et al. (2012)
Er-27	Central activity	Ashes on NW cliff of Enclos Fouqué (Bellecombe cliff)	Ash bed	Ashes draping the lower third of the Enclos Fouqué cliff	1	–380	100							–
Er-28	Central activity	Ashes near the “Gîte du Volcan” (“Cendres de Bellecombe” in B’81 and V&B’82)	Ash beds	Sampled near the Gites du Volcan	–178	–597	86	–680	–755	8.7	–607	–671	5.4	Bachèlery (1981)
Er-28	Central activity	Partage Tephra (Unit 2; CC1 layer)	Ash bed	Section 6 (Partage cliff)	–366	–490	99.2	–501	–506	0.8				Di Muro et al. (2012)
Er-28	Central activity	Ashes near the “Gîte du Volcan”	Ash beds	Upper part of an ash bed. below a bed of scoriae	–357	–784	97.5	–255	–283	1.9	–235	–246	0.6	–
Er-28?	N120	Piton des Tangues tephra (Below Red Tephra Unit)	Lapilli bed?	Ash or lapilli bed above the Upper Bellecombe ash	608	–2345	100							Abchir (1996), pg. 86
Er-29	Central activity	Partage Tephra (Unit1; CC0 layer)	Ash bed	Section 6 (Partage cliff)	–919	–1121	100							Di Muro et al. (2012)

(continued)

**Table 8.1** (continued)

Eruption ID	Location	Unit name	Unit type	Note on the sample	Calibrated probability distribution (A.D.)–Max probability 2σ			Calibrated probability distribution (A.D.)–Secondary probability 2σ			Calibrated probability distribution (A.D.)–Tertiary probability 2σ			Reference
					Min age	Max age	% prob.	Min age	Max age	% prob.	Min age	Max age	% prob.	
REU140825-PDT2	N120	Near Piton des Tangués parking	Ash beds	Black soil below red tephra lapillis covering Bellecombe falls	–1020	–1211	100							This chapter
Er-30	Central activity	Upper unit of Bellecombe ash	Ash bed	Sample REU 1303-07 A1	–1228	–1411	100							This chapter
Er-31	N120	Piton Sauvetage	Strombolian cone	Ash bed	–1152	–1501	97.7	–1127	–1150	2.3				Bachelery (1981)
Er-32	Central activity	Upper unit of Bellecombe ash	Ash bed	Sample REU 1303-07 A2 2A	–1280	–1428	100							This chapter
Er-33	N120	Langevin plateau fall- bed 6	Ash and lapilli bed	Section 1—Caldera des Sables cliff	–1284	–1431	100							Di Muro et al. (2012)
Er-34	Central activity	Upper unit of Bellecombe ash	Ash bed	Sample REU 1303-07 A2 2C/1 km west of Piton des Basaltes	–1288	–1437	100							This chapter
Er-41	Central activity	Lava3 of W Enclos Fouqué rim	Lava flow	Sample RE-90-15b (below Bellecombe ash); oceanite										–
REU140822-2	N120	0.5 km from Nez de Bœuf, above Bellecombe ash fall	Ash beds	Soil above Bellecombe and below a thin lapilli layer	–1371	–1457	69.8	–1300	–1359	27	–1477	–1494	3.2	This chapter
Er-41	Central activity	Lava3 of W Enclos Fouqué rim	Lava flow	Sample RE-90-15a (below Bellecombe ash); oceanite										–
Er-35	N120	Piton des Tangués ashes ; Upper Bellecombe ash (U3a)?	Ash bed	Cpx-gabbro rich ash bed (above Piton des Tangués cone; Below Red Tephra Unit)	–1288	–1643	99.9	–1655	–1656	0.1				–
Er-35	N120	Ashes near commerson (below red tephra unit)	Ash bed	Fine ash bed near commerson	–1411	–1615	100							Bachelery (1981)
Er-42	Central activity	Lava2 of NW Enclos Fouqué rim	Lava flow	Sample RE-90-31 (below partage unit)										–
Er-36	N120	Piton des Basaltes	Strombolian cone	Scoriae bed	–1492	–1694	93.6	–1453	–1482	4	–1716	–1735	2.3	–
Er-37	Central activity	Bellecombe ash; upper bellecombe ash (U3a?)	Ash bed	Sample REU 1303-07 A6/About 1 km east of Piton dans l'bout	–2029	–2155	81.5	–2157	–2200	18.5				This chapter
Er-37	Central activity	Piton des Tangués ashes; upper Bellecombe ash (U3a)?	Ash beds	Cpx-gabbro rich ash bed (above Piton des Tangués lava; below red Tephra unit)	–1920	–2369	94.2	–2417	–2456	2.9	–2373	–2408	2.9	–
Er-43	Central activity	Lava1 of W Enclos Fouqué rim	Lava flow	Sample RE-90-24a										–

(continued)

**Table 8.1** (continued)

Eruption ID	Location	Unit name	Unit type	Note on the sample	Calibrated probability distribution (A.D.)–Max probability 2σ			Calibrated probability distribution (A.D.) –Secondary probability 2σ			Calibrated probability distribution (A.D.)–Tertiary probability 2σ			Reference
					Min age	Max age	% prob.	Min age	Max age	% prob.	Min age	Max age	% prob.	
Er-43	Central activity	Lava1 of W Enclos Fouqué rim	Lava flow	Sample RE-90-25										–
AND 02/ REU140721/ S3b	N120	Trous Blanc site (S3b ash below Bellecombe and above Trous Blanc eruption)	Ash beds	Charcoals at the base of S3B yellow layer (unit just below Bellecombe fall)	–2577	–2764	73.5	–2804	–2865	26.2	–2770	–2773	0.3	This chapter
Er-38	Central activity	Lower Bellecombe ash Unit (U1b)	Ash beds	Fossil wood (unburned)	–2336	–3110	97.9	–3237	–3266	0.8	–3293	–3316	0.6	Abchir (1996), pg. 86
AND 04/ REU140723-1/ S3b	N120	Piton Sec (S3b ash below Bellecombe)	Ash beds	Charcoals at the base of S3B yellow layer (unit just below Bellecombe fall)	–2917	–3098	99.1	–3254	–3261	0.9				This chapter
AND 08/ REU140728-2a/ bglaBR	N120	Trous Blancs site; top of the Trous Blancs Breccia	Ash beds	Charcoals at the base of L2(?) orange red layer (unit just below Bellecombe fall)	–3370	–3477	68.9	–3482	–3525	23.7	–3600	–3625	7.4	This chapter
AND 12/ REU140801-2	N120	At the feet of Nez de Bœuf spatter (below Bellecombe)	Ash beds	Soi below thin lapilli; layer just below Bellecombe fall	–3370	–3476	60.7	–3483	–3532	23.4	–3582	–3629	15.9	This chapter
Er-39	Central activity	Lava2 of NW Enclos Fouqué rim	Lava flow	Basal scoriae below the uppermost lava flow near Bellecombe (below Partage unit)	–3263	–3794	92.3	–3100	–3246	7.7				Bachélery (1981)
Er-40	Central activity	Second unit of Bellecombe ash	Ash bed	Sample REU 1303-07 A2 2b/1 km west of Piton des Basaltes	–3634	–3713	97.2	–3540	–3556	1.6	–3743	–3758	1.3	This chapter
Er-43	Central activity	Lava1 of W Enclos Fouqué rim	Lava flow	Sample RE-90-24b; oceanite										–
AND 02/ REU140721/ S3a	N120	Trous Blancs area	Ash beds	S3a ashes above the Trous Blanc eruption	–4227	–4341	89.5	–4167	–4202	7.8	–4077	–4095	2	This chapter
REU140825-PDT1	N120	Piton des Tangués parking	Ash beds	Thick red lahar below Bellecombe falls	–4346	–4460	100							This chapter
Er-44	Piton des Neiges?	Grand Etang deep drilling	Conglomerate	Fossil wood (unburned) in conglomerates at the base of the Puy de l'Etang ashes	–4352	–4800	99.7	–4819	–4823	0.3				Banton (1985)

(continued)

**Table 8.1** (continued)

Eruption ID	Location	Unit name	Unit type	Note on the sample	Calibrated probability distribution (A.D.)–Max probability $2\sigma$			Calibrated probability distribution (A.D.)–Secondary probability $2\sigma$			Calibrated probability distribution (A.D.)–Tertiary probability $2\sigma$			Reference
					Min age	Max age	% prob.	Min age	Max age	% prob.	Min age	Max age	% prob.	
Er-45	N120	“Les Trous Blancs” lava field	Lava flow											Villeneuve and Bachelery (2006)
Er-46	N120	Ashes along the path to “Piton des Tangues”	Ash beds	Section 12; layer 5 (above the “Cendres de Notre Dame” unit)	–5745	–5918	93.4	–5950	–5975	6.6				Di Muro et al. (2012)
Er-47	N120	Piton textor	Ash beds		–5740	–6231	100							Bachelery (1981)
Er-48	N120	Ashes between Piton textor and Piton des Cailles	Ash beds		–6611	–7060	100							Bachelery (1981)
AND 04/ REU140723-1/ S3a	N120	Trous Blancs area (near Piton sec; above Trous Blancs eruption)	Ash beds	S3a ash layer	–6752	–7051	98.7	–6709	–6720	1.3				This chapter
Er-49	N120	Piton dans le bout	Strombolian cone		–8254	–9223	100							Bachelery (1981)
AND 06/ REU140723-3/ S3b	N120	near Piton Sec (S3b ashes above the Trous Blanc eruption)	Ash beds		–8597	–8823	99.2	–8572	–8565	0.8				This chapter
Er-50	Piton des la Fourmaise?	Grand Etang deep drilling	Conglomerate	Fossil wood in conglomerate below the deep lavas (–40 m) met by the drill	–10,427	–10,801	96.2	–10,287	–10,339	2	–10,350	–10,396	1.5	Banton (1985)
REU031014-1BC	Piton des Neiges	Bras des Lianes			–11,802	–12,111	100							This chapter
Er-51	Central activity	Notre Dame de la Paix -2	Ash beds		–12,873	–19,716	100							–
LAS 17/ REU140718-1/ Part B	N120	Bois Court lava flow	Lava flow		–19,222	–19,908	100							This chapter
LAS 17/ REU140718-1/ Part A	N120	Bois Court lava flow	Lava flow		–19,347	–19,948	100							This chapter

(continued)

**Table 8.1** (continued)

Eruption ID	Location	Unit name	Unit type	Note on the sample	Calibrated probability distribution (A.D.)–Max probability 2σ			Calibrated probability distribution (A.D.) –Secondary probability 2σ			Calibrated probability distribution (A.D.)–Tertiary probability 2σ			Reference
					Min age	Max age	% prob.	Min age	Max age	% prob.	Min age	Max age	% prob.	
LAS 17/ REU140718-1/ Part C	N120	Bois Court lava flow	Lava flow		–19,507	–20,114	100							This chapter
Er-52	Central activity	“Cendres de Notre Dame” Unit	Ash beds											
Er-53	N120	Bois court	Strombolian cone	Altered ash layer. below the lava flow	–20,540	–21,776	100							–
Er-54	Central activity	Plaine des Sables caldera fault	Caldera fault	Sample RE-90-07; surface of the caldera fault										–
Er-55	N120	Piton Manuel—Piton des Cabris	Strombolian cone											–
Er-56	Central activity	Notre Dame de la Paix -1	Ash beds		–36,591	–42,016	100							–
Er-57	N120 SVZ	Piton Rouge (St. Joseph)	Strombolian cone											–
Er-58	Central activity	Summit lava of the Plaine des Ramparts	Lava flow	Sample RE-90-06; last lavas of the caldeira										–
Er-59	Central activity?	Submarine tephra (S17-656 drill)	Ash bed	Sample R4-1; basaltic ash										Fretzdorff et al. (2000)

Abbreviation: *EF* Enclos Fouqué; *CLEF* Enclos Fouqué Lava Field; *RZSE* SE rift zone; *RZNE* NE rift zone; *N120* NW rift zone

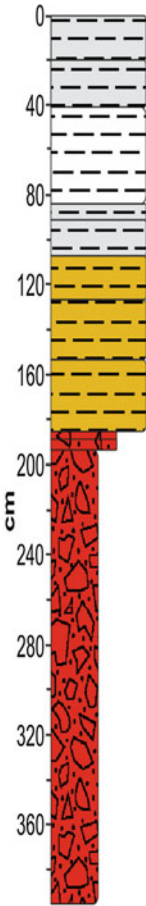


**Table 8.2** GDE core description and coarse ash (710 <  $\phi$  < 1000  $\mu$ m) optic microscope analysis

CORE: GDE		Coarse ash					
DEPTH:	623 cm	cm	ol	pl	px	qz	mt
	0-46	Fine ashes fine dark grayish (0-14 cm) to reddish (14-36 cm) and yellowish (36-46 cm) brown ashes. Coarse sand fraction increase toward the base					
	46-59	poorly sorted layer of lithics ( $\phi=5$ mm) and altered scoriae ( $\phi=2-3$ cm) within an abundant mostly fine matrix	X				
	59-87	fine ash. A 6 cm thick cobble at 65 cm					
	87-96	poorly sorted lapilli and gravels within a fine matrix					
	96-106	fine ash with few coarse ash					
	106-168	fine matrix with very poorly sorted scoriae and gravels					
	168-176	fine ash					
	176-179	pebbles and scoriae within fine ash					
	179-200	vesicular dark lavas					
	200-207	light brown clay					
	207-214	lava					
	214-347	yellowish brown clay with some very altered scoriae and rounded gravel ( $\phi=4-10$ mm). At 251-255 cm black lapilli ( $\phi=5$ mm) within a coarse matrix, at 320-321 black lapilli ( $\phi=5$ mm) within a fine matrix					
	347-350	Proximal Scoria altered lapilli ( $\phi=5$ mm; $\phi_{\max}<1$ cm) surrounded by an orange (at the top) to dark matrix					
	350-362	yellowish brown clay with some very altered scoriae and rounded gravel.					
	362-371	lapilli and lithics surrounded by a fine to coarse matrix					
	371-378	lava					
	378-381	lapilli and gravel surrounded by a brown poorly sorted matrix					
	381-397	very poorly sorted lapilli ( $\phi_{\max}<2.5$ cm) within an orange (381-387 cm) to dark (387-397 cm) matrix					
	397-409	fine reddish light brown ash					
	409-623	very poorly sorted scoriae ( $\phi<5$ cm) with some to scarce matrix. Lavas at 476 and 494 cm					
		cm	ol	pl	px	qz	mt
		3					
		10					
		21					
		34					
		41					
		53	X				
		63	X				
		78	x				
		88					
		92					
		105					
		123					
		166					
		170					
		205					
		230					
		275					
		330					
		349					
		353					
		384					
		404					
		cm	v	$\mu$ xx	xx	ag	
				lth			
		3					X
		10					X
		21					X
		34					X
		41					X
		53					X
		63					X
		78					X
		88					X
		92					X
		105					X
		123					X
		166					X
		170					X
		205					X
		230					X
		275					X
		330					X
		349					X
		353					X
		384					X
		404					X

*Legend* Stratigraphic log: *G* gravel; *GS* gravel and sand; *S* sand; *C* Clay; *R* coherent rock. Microscopic analysis: *ol* olivine; *pl* plagioclase; *px* pyroxene; *qz* quartz; *mt* magnetite; *v* glass;  $\mu$ xx microcrystalline; *xx* crystals; *ag* fine sand aggregates; *lth* lithics/lava fragments (as part of  $\mu$ xx). Quantities: *x* abundant/frequent; *x* some; *x* few; *tr* trace

**Table 8.3** PDE2core description and coarse ash (710 <  $\phi$  < 1000  $\mu\text{m}$ ) optic microscope analysis

CORE:	PDE2	Coarse ash						
DEPTH:	395 cm	cm	ol	pl	px	qz	mt	
	cm	<b>Fine Ashes</b>						
	0-20	dark fine ash with many roots						
	20-27	dark gray fine ash with few achnelith lapilli $\phi_{\text{max}} < 1 \text{ cm}$						
	27-41	reddish dark gray fine ash with few achnelith lapilli $\phi_{\text{max}} < 5 \text{ mm}$						
	<b>Bellecombe Ashes</b>							
	41-84	grayish brown fine ash with few granule, sometimes forms aggregates						
	<b>Fine Ashes</b>							
	84-91	brown fine ash						
	91-107	dark brown fine ash						
	<b>Soil</b>							
	107-127	reddish clay with few coarse sand and altered scoriae $\phi_{\text{max}} < 1 \text{ cm}$						
	127-153	light brown ash with a flat and rounded 2 cm thick scoria, rare granule						
	153-185	reddish brown ash with few granule (at the top) and some altered scoria ( $\phi_{\text{m}} = 1 \text{ cm}$ ; $\phi_{\text{max}} < 4 \text{ cm}$ ). A 3 cm thick lava fragment at 155 cm						
	<b>Proximal deposit</b>							
	185-189	dark altered scoria ( $\phi_{\text{m}} = 1.2 \text{ cm}$ ; $\phi_{\text{max}} < 4 \text{ cm}$ ) and matrix						
	189-194	matrix sustained yellowish brown layers with altered lapilli $\phi_{\text{max}} < 1 \text{ cm}$						
	194-395	very poorly sorted scoria layer $\phi_{\text{max}} < 4 \text{ cm}$ . A yellowish matrix decrease from the top to base						
		cm	v	$\mu\text{xx}$	xx	ag		
				lth				
		23	x				X	
		35	x	x	x	tr	X	
		49	tr	tr	x	x	X	
		80		x	X	x	X	
		88		x	x	x	X	
		97		X	x	x	X	

*Legend* Stratigraphic log: *G* gravel; *GS* gravel and sand; *S* sand; *C* Clay; *R* coherent rock. Microscopic analysis: *ol* olivine; *pl* plagioclase; *px* pyroxene; *qz* quartz; *mt* magnetite; *v* glass;  $\mu\text{xx}$  microcrystalline; *xx* crystals; *ag* fine sand aggregates; *lth* lithics/lava fragments (as part of  $\mu\text{xx}$ ). Quantities: *x* abundant/frequent; *x* some; *x* few; *tr* trace

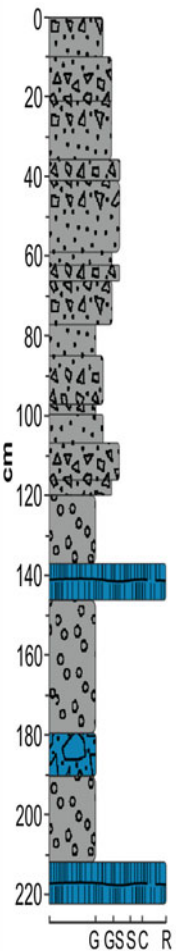


**Table 8.5** PDS2 core description and coarse ash ( $710 < \phi < 1000 \mu\text{m}$ ) optic microscope analysis

CORE: PDS2 DEPTH: 243 cm		Coarse ash					
		cm	ol	pl	px	qz	mt
<b>Reworked lapilli and ashes</b>							
0-4	black fine lapilli ( $\phi_m = 2 \text{ mm}$ ; $\phi_{max} = 5 \text{ mm}$ ) with abundant dark matrix. Rare red lapilli	7	X				
		14	X				
		20	X				
		22	X				
		26	X				
		32	X				
4-10	black fine lapilli ( $\phi_m = 5 \text{ mm}$ ) with yellowish ash	41	X				
10-18	black lapilli ( $\phi_m = 5 \text{ mm}$ ; $\phi_{max} = 8 \text{ mm}$ ) more granular at the base. Scarce matrix. Rare red lapilli	47	X		tr		
		67	X				
18-21	well sorted lapilli ( $\phi_m = 5 \text{ mm}$ )	72	X				
21-30	very fine lapilli. Coarse ash fraction increase toward the base. Rare red lapilli. Some Olivine crystals in the lower part	99	X				
		124	X				
		126	X	x	tr		x
		128	X				
30-33	fine lapilli without matrix	135	X	x		tr	tr
33-42	normally graded lapilli bed (from $\phi_m = 2 \text{ mm}$ to $\phi_m = 5-8 \text{ mm}$ )	140	X		tr		tr
		148	X				
42-68	black fine lapilli ( $\phi_m = 2-5 \text{ mm}$ ). Coarse ash augmentation toward the top. Some olivine crystals. Rare red lapilli	163	X	x		tr	
		176	X	x	tr	tr	
		194	X	x			
		201	X				
		211	X				
<b>Black Lapilli</b>							
68-125	black well sorted ( $\phi_m = 5-10 \text{ mm}$ ; $\phi_{max} < 2 \text{ cm}$ ), achnelith and vesicular lapilli. Slight reverse grading. A 3 cm thick olivine bearing lava fragment at the base. The lapilli layer has a very thin ( $< 1 \text{ mm}$ ) coarse ash layers at the base	cm	v	$\mu\text{xx}$ lth		xx	ag
		7	X			x	
		14	X	tr		x	
		20	X			x	
		22	X	tr		x	
		26	X	tr		x	
		32	X	tr		x	
		41	X	tr		x	
		47	X	tr		x	
		67	X	tr		x	
		72	X			x	
		99	X			x	
		124	X	x	x	x	
		126	x	x	x	X	X
		128			x		X
		135	x	x	x	X	
		140	x	x	tr	x	
		148	x	x	tr	x	
		163	tr	X	X	X	
		176	tr	X	X	X	
		194		X	X	X	
		201	tr	X		x	
		211	X	x		X	
<b>Bellecombe ashes</b>							
125-126.5	brown olivine-bearing fine ash						
126.5-130	grayish brown fine ash with few granule						
130-198	Coarse olivine-bearing scoriaceous and partially altered lava fragments ( $\phi_{max} < 5 \text{ cm}$ ) surrounded by fine grayish ash that forms aggregates. Sometimes the gray matrix is replaced by a fine red-brown ash (132-133 and 136-142 cm) or by a reddish dark coarse ash (142-151 cm)						
<b>Pre-Bellecombe deposits</b>							
198-204	dark scoriaceous lava fragments ( $\phi_{max} < 2 \text{ cm}$ ) and some coarse ash						
204-215	poorly sorted red lapilli ( $\phi_{max} < 1 \text{ cm}$ ) and spatter bombs ( $\phi_{max} < 4 \text{ cm}$ ). Scarce matrix						
215-243	poorly sorted dark, scoriaceous lava fragments ( $\phi_{max} = 1-3 \text{ cm}$ ) and few red matrix and lapilli which decrease towards the base						

*Legend* Stratigraphic log: *G* gravel; *GS* gravel and sand; *S* sand; *C* Clay; *R* coherent rock. Microscopic analysis: *ol* olivine; *pl* plagioclase; *px* pyroxene; *qz* quartz; *mt* magnetite; *v* glass;  $\mu\text{xx}$  microcrystalline; *xx* crystals; *ag* fine sand aggregates; *lth* lithics/lava fragments (as part of  $\mu\text{xx}$ ). Quantities: *x* abundant/frequent; *x* some; *x* few; *tr* trace

**Table 8.6** PDS1 core description and coarse ash ( $710 < \phi < 1000 \mu\text{m}$ ) optic microscope analysis

CORE: PDS1		Coarse ash					
DEPTH:	222 cm	cm	ol	pl	px	qz	mt
	0-10	fresh black lapilli ( $\phi_m = 2-5$ mm; $\phi_{max} < 8$ mm) and few coarse ash. Slightly normal grading. Some oxidized red lapilli	12	X			
	10-36	fresh black lapilli ( $\phi_m = 2-5$ mm; $\phi_{max} < 8$ mm) and coarse ash. Slightly normal grading. Some oxidized red lapilli	28	X			
	36-41	Fine lapilli ( $\phi_m = 2-5$ mm) and abundant yellowish matrix. Coarse olivine-bearing ash and granule at the roof	36	X			
	41-66	fine lapilli ( $\phi_m = 2-5$ mm but coarser at the roof and at the base $\phi_m = 5-10$ mm). Abundant coarse matrix, decreasing at the base. Some red lapilli	39	X			
	66-97	fine lapilli with reverse grading ( $\phi_m = 5$ mm to 2 mm at the base). Matrix in the superior part. Some red lapilli	43	X			
	97-100	well sorted lapilli ( $\phi_m = 5$ mm). Some red lapilli	54	X			
	100-120	normal graded lapilli layer ( $\phi_{max} < 5$ mm to 10 mm at the base) with decreasing ash toward the base	64	X			
	120-137	well sorted black, fresh and vesicular lapilli ( $\phi = 5-8$ mm; $\phi_{max} < 1.5$ cm)	70	X			
	137-146	very vesicular fresh olivine basalt; slightly reddish oxidation; few ol crystal	77	X			
	146-180	massive well sorted black fresh and vesicular lapilli; $\phi = 5-8$ mm $\phi_{max} < 1.5$ cm	80	X			
	180-190	vesicular basalt; slightly reddish oxidation	88	X			
	190-212	massive well sorted black, fresh and vesicular lapilli ( $\phi = 8-10$ mm; $\phi_{max} < 1.5$ cm)	98	X			
	212-222	vesicular basalt; slightly reddish oxidation	102	X			
			116	X			
			122	X			
			132	X			
			151	X			
			162	X			
			174	X			
			192	X			
			202	X			
			211	X			
		cm	v	$\mu\text{xx}$	xx	ag	
				lth			
			12	X	tr	x	
			28	X	x	x	
			36	X	tr	x	
			39	X	tr	x	x
			43	X	x	tr	x
			54	X		x	
			64	X		x	
			70	X		x	
			77	X		x	
			80	X		x	
			88	X	tr	tr	x
			98	X		tr	x
			102	X		x	
			116	X		x	
			122	X		x	
			132	X	tr	x	tr
			151	X		x	
			162	X	x		
			174	X	tr	x	
			192	x	x	x	x
			202	x	X	X	x
			211	x	X	X	x

*Legend* Stratigraphic log: *G* gravel; *GS* gravel and sand; *S* sand; *C* = Clay; *R* coherent rock. Microscopic analysis: *ol* olivine; *pl* plagioclase; *px* pyroxene; *qz* quartz; *mt* magnetite; *v* glass;  $\mu\text{xx}$  microcrystalline; *xx* crystals; *ag* fine sand aggregates; *lth* lithics/lava fragments (as part of  $\mu\text{xx}$ ). Quantities: *x* abundant/frequent; *x* some; *x* few; *tr* trace

a synthesis of all macroscopically and microscopically performed observations performed on drilling cores is presented.

In order to better constrain the explosive activity and the stratigraphic correlations in the N120 rift zone, the excavation of about 30 tephra sections has been performed in the proximal and middle sector of the volcano. It leads to the identification of several, spatially limited, lapilli deposits, and of three major tephra sequences, respectively in the Piton de Partage, Plaine des Sables, and Plaine des Remparts sectors (Fig. 8.1). These three sequences are described in the following.

### 3.1 The Partage Tephra

The “Partage Tephra” (Fig. 8.3) is here defined for the first time. It consists in a <1.5 m thick sequence of ash, lapilli and scoria beds that drape almost continuously the northern wall of the Enclos Fouqué caldera. The sequence attains the maximum thickness close to the northern caldera rim,

thins out quickly when moving westward in the Plaine des Sables and is not observed in the Fond de la Rivière de l’Est, neither in more distal areas, as on the Plaine des Remparts plateau. The tephra sequence underlies the modern soil and has been divided in three units (U1; U2; U3 from base to top), on the basis of grain size, componentry and  $^{14}\text{C}$  age. This tephra sequence was initially included in the “Bellecombe ash unit”, but it results to be younger. Thin, usually <2 cm-thick, laterally continuous charcoal-rich layers are widespread inside the “Partage Tephra” sequence. The lowermost layer (CC0:  $2855 \pm 35$  BP) occurs in the middle of Unit 1, while the others, CC1 and CC2, occur respectively at the base of Unit 2 (CC1:  $2340 \pm 30$  BP) and of Unit 3 (CC2:  $2140 \pm 35$  BP) (Table 8.1).

Near the Enclos Fouqué cliff, Unit 1 (U1) overlies a thin, usually <0.5 m thick bed of matrix-supported breccia containing scattered angular decimeter-sized lithic clasts (“Bellecombe breccia” sensu Bachèlery 1981). In more distal areas, Unit 1 often overlies older lavas. In

#### Partage Tephra sequence

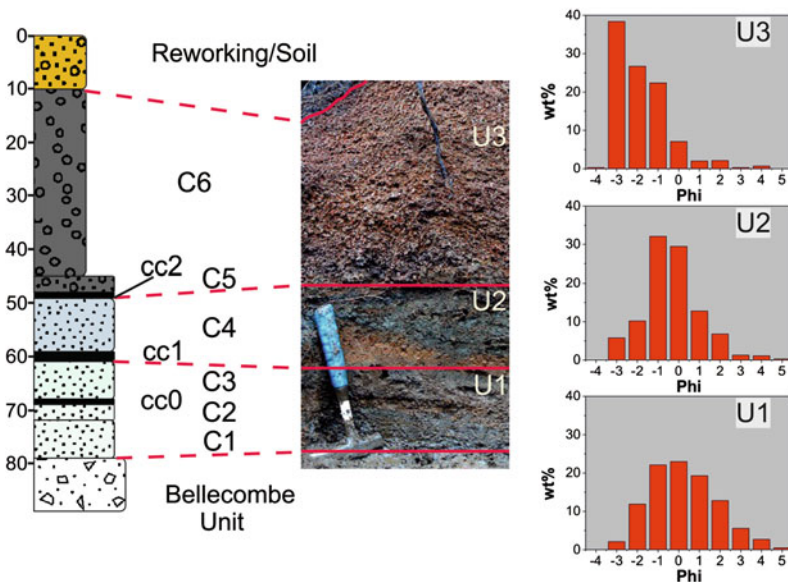


**Fig. 8.3** “Partage Tephra” sequence. C1, C2, C3 fine ash (U1); C4 coarse ash (U2); C5 lapilli and ash, C6 well-sorted lapilli bed (U3); cc0, cc1, cc2 charcoal-rich layers (respectively dated to 2855, 2340 and

2140 year BP; Table 8.1). Average grain size distribution for each Unit is plotted as histogram. The matrix-supported breccia underlying the “Partage Tephra” sequence is attributed to the “Bellecombe Unit”



the most proximal outcrops, Unit 1 groups at least four cm thin ash layers, whose maximum global thickness ( $\approx 30$  cm) is observed close to Piton de Partage site. Piton de Partage scoria cone lies below Bellecombe breccia and “Partage” ashes. U1 ashes are brown to pink colored, fine grained ( $Md_{\phi} < -1.5 \phi$ ) and poorly sorted ( $\sigma_{\phi} = 1.5-2 \phi$ ) (Fig. 8.3). The ash layers are composed of minor highly fluidal glassy juvenile clasts in a volumetrically dominant matrix formed by variably altered lava fragments, possible small gabbro clasts, olivine crystals and rare euhedral quartz and magnetite (mostly in the lowermost layers). Similarities (in terms of grain size and componentry) between Unit 1 of the “Partage Tephra” and the (older) “Bellecombe Ash unit” suggest the possibility of an analogous mechanism at the origin of these deposits.

Unit 2 (U2) is a grey homogeneous lapilli and ash bed ( $Md_{\phi} = -1 \phi$ ), moderately sorted ( $\sigma_{\phi} = 1-1.5 \phi$ ), with a high amount of dense clasts (mm- to cm-sized grey lava fragments) (Fig. 8.3). Coarse fragments are dispersed in a fine-grained ash matrix containing olivine crystals and rare fluidal glassy fragments, whose amount increases towards the top of the bed. Bed thickness changes between 6 and 12 cm along the outcrop area.

Unit 3 (U3) consists of two scoria-rich beds. In the lower and thinner bed ( $< 5$  cm thick), reddish scoriae are supported by an ashy matrix. The upper main bed is a clast-supported deposit of mm- to cm-sized, reddish, variably altered scoriae with a moderate to low amount of crystals and lithic fragments. The bed is weakly normally graded ( $Md_{\phi} = -3$  to  $-2 \phi$ ;  $\sigma_{\phi} = 1-2 \phi$ ). The amount of free olivine crystals increases from the base to the top of the bed. The maximum thickness (1 m) is observed on the Enclos Fouqué wall located in front of the Formica Leo cone and decreases quickly moving away from this location, suggesting a quite narrow isopachs distribution. At Piton de Partage, the U3 thickness is about 35 cm.

The thickness distribution of the “Partage Tephra” sequence strongly supports the emission from one or more sources located close and (at least for U1 and U2 eruptions) inside the Enclos

Fouqué. Eruptive dynamics possibly evolve from phreatomagmatic in the lowermost units (U1 and U2) to magmatic in the upper one (U3). U2 bed drapes the inner cliffs of Enclos Fouqué and gives a minimum age to the formation of this depression.

## 3.2 The Plaine des Sables Black Tephra

The black pyroclastic blanket forming the surface of large part of the Plaine des Sables consists mainly of very fresh and vesicular, fine to medium achnelith and black lapillis, which cover the areas surrounding between Piton Chisny and Piton Haüy cones. We have referred to this deposit as “Black Tephra” unit. It shows a maximum thickness of about 2.5 m in the area between Piton Chisny and Demi-Piton cones, near the NW foot of Piton Chisny edifice (Fig. 8.4). The deposit is absent on the Enclos Fouqué rim, while it is still present, although less than 10–20 cm thick, on the west edge of the Plain des Sables. In the proximal area, the “Black Tephra” sequence is a crudely stratified, well-sorted lapilli bed. Locally, a thin and coarse ash layer can be observed at its base (S13 and S20) that vanishes quickly when moving outside the main dispersal axis. In PDS2 core the basal ash layer is almost absent. In the proximal facies, the S20 section shows the presence of some spatter bomb layers. The distal facies (S3 section) is instead characterized by a basal coarse ash, a middle well sorted lapilli body, and a lapilli and ash top layer. Whereas not overlain by lavas, the deposit is often largely reworked (as in PDS1 and PDS2). In the ash fraction, olivine is the only mineral phase. Moving northwards in the Plaine des Sables, the Chisny black lapilli layer overlies the yellowish lapilli layer related to Piton Haüy activity. A dm to m thick bed of reworked ash and lapillis occur between them.

## 3.3 The “Red Tephra”

In the Plaine des Remparts area, the most widespread deposit consists in a bed of reddish glassy fluidal scoriae, here named “Red Tephra” unit,

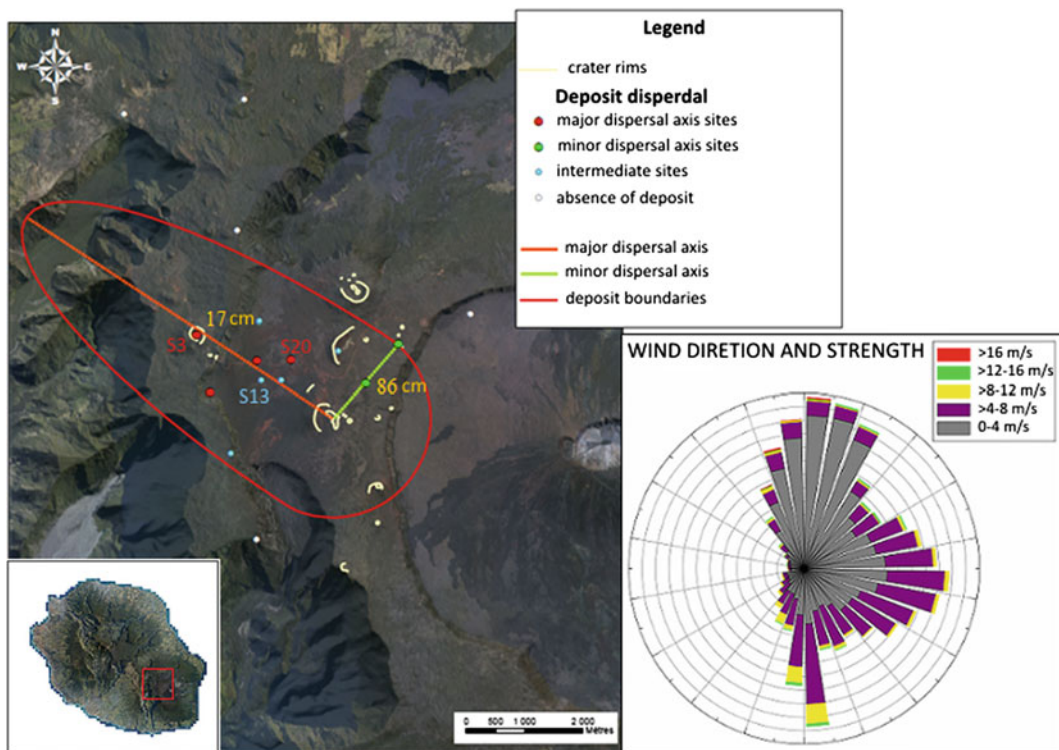


**Fig. 8.4** “Black Tephra” unit maximum dispersal. S3, S13 and S20 are the sites whose logs are shown in Fig. 7.5 . Wind strength and direction records at Pas de

Bellecombe between 01/09/2007 and 15/03/2011 are reported in the down right corner (source Météo France)

cropping out between Piton de l’Eau cone and Commerson crater. Maximum thickness (up to 2.5 m) is observed close to Piton des Cailles. Near Piton des Tangues, the fall bed is separated by a decimeter-thick black soil from the underlying Bellecombe Ash unit. The Red Tephra is restricted to the middle-distal sectors and is not observed in the proximal area of Plaine des Sables. As a whole, this unit has not been characterized yet and the source vent is unknown.

#### 4 Frequency of Pdf Explosive Activity During the Last 4000 Years

Available ages of Pdf pre-historic volcanic events, together with new  $^{14}\text{C}$  dating (Centre de Datation par le Radiocarbène, University Lyon 1),

are here reviewed in order to identify the main periods of recent explosive volcanic activity (Table 8.1).

The main tephra identified all around the Enclos Fouqué is the “Bellecombe Ash unit”. It corresponds to a complex sequence of ash, crystal and lithic-rich deposits (Bachelery 1981; Mohamed-Abchir 1996). This deposit is thought to be emplaced during violent phreatic/phreatomagmatic events related to the flashing of an extensive hydrothermal system during the collapse of the Enclos Fouqué caldera (Bachelery 1981; Mohamed-Abchir 1996; Fontaine et al. 2002; Upton et al. 2000).

The ages of the caldera formation and related Bellecombe Ash unit are poorly constrained. They are likely comprised in a time span ranging between the emplacement of the lavas forming the uppermost part of the Enclos Fouqué walls

that underly Bellecombe and Partage ashes ( $4745 \pm 130$  BP,  $3340 \pm 1012$ ; respectively Er-39 and Er-41 in Table 8.1) and that of the crystal and lithic-rich Bellecombe and Partage ashes themselves (several ages between  $4175 \pm 145$  and  $2320 \pm 90$  BP; respectively Er-38, which matches the Bellecombe Ash type-section at the Petite Carrière outcrop, and Er-28 in Table 8.1). Interestingly, Vergnolle and Bachélery (1982) report that ashes with an age of  $2140 \pm 80$  BP (U3 of the “Partage Tephra” sequence, in this paper) drape the lower and inner wall of Bellecombe cliff. This possibly represents the upper age for a series of caldera-forming events.

Most of the eruptive products, lavas and tephtras, cropping out inside the Enclos Fouqué caldera are much younger than 2320 BP, actually younger than 1750 CE (Table 8.1), final age of the widespread pāhoehoe lava field named CLEF by Lénat et al. (2001). Notable exceptions are the central cone and small scoria cones, like Formica Leo and Puy Mi-côte (Fig. 8.1), of unknown age, but covered by the CLEF pāhoehoe lava field.

Recent and detailed stratigraphic analysis of the 340 m high walls of the summit PdF caldera (Peltier et al. 2012; Michon et al. 2013) failed in identifying deposits that could be related to major summit explosive events. Michon et al. (2013) highlight that the summit cone evolution is mainly made by the alternation of crater collapse, lava infilling and outpouring episodes, suggesting a dominant effusive magmatic style punctuated by mild to weak explosive events unable to leave significant and durable traces on the territory. Moreover, the span of time covered by these processes is probably short (Michon et al. 2013). For instance, caldera filling appears to be relatively rapid. The ca. 300 m-deep, 600 m-across 1931 summit collapse structure was filled in 2006, just before the major 2007 summit collapse event. This recent and dominantly effusive activity of PdF was preceded by an important strombolian to hawaiian activity, whose remnants is a basal cone made of red to ochre scoriae visible at the bottom of the present Dolomieu crater (Michon et al. 2013). Both hawaiian, strombolian and possible phreatomagmatic deposit have been recognized in this lower sequence (Unit 1a and 1b in Peltier et al. 2012; U1a

in Michon et al. 2013) at an elevation corresponding to the Enclos Fouqué caldera filling. The deposits related to this explosive phase of unknown age have not been identified outside the Enclos Fouqué (Peltier et al. 2012; Michon et al. 2013).

Weak to mild explosive eruptions related to the central activity have left very little stratigraphic record, except near the summit cone (Michon et al. 2013). For instance, fine ash and Pele’s hairs of the 2007 caldera forming event have been quickly eroded away and only little traces are found inside the Bory crater, just 6 years after the event. The deposits of the most intense recent explosive eruptions (1961 and 1860) are only found near the volcano summit.

A notable exception is represented by the “Partage Tephra” sequence. Our new datings clearly indicate that the “Partage Tephra” sequence groups the deposits of several eruptions, which have occurred after a main event of breccia formation. These eruptions occurred in a relatively long period ( $-1124$  to  $-52$  BC; Table 8.1) and possibly represent an unusually violent series of events occurring soon after (and partially associated with) the last phase of Enclos Fouqué caldera collapse. These deposits give thus a lower limit for the age of the PdF central cone.

Along the N120° rift zone, the “Red Tephra” unit seems to pertain to a similar age interval. In this area, two  $^{14}\text{C}$  ages ( $3735 \pm 90$  and  $3205 \pm 75$  BP; respectively Er-37 and Er-35 in Table 8.1) are reported bracketing the underlying Bellecombe cpx-gabbro rich ash. Very similar ages ( $3715 \pm 30$  and  $3220 \pm 50$  BP) were also found 1 km East from Piton dans le Bout (Er-37, Table 8.1) and in an ash bed underlying the Red Tephra near Commerson crater (Er-35, Table 8.1). The widespread presence in this sector, up to the Caldera des Sables rim (Er-30 to Er-36 in Table 8.1), of ash beds belonging to the “Bellecombe Ash unit” provide hence a upper limit for the age of the Red Tephra.

All tephra units identified in the period succeeding the “Partage” and “Red” tephra sequences have a very limited degree of dispersion. For instance, Er-21 and Er-20 new radiocarbon ages, respectively dated to  $868 \pm 30$  and  $620 \pm 30$  BP,

identify two relatively recent and very localized events occurred close to Langevin area, inasmuch their deposits are absent both within the near Plaine des Sables (PDS2 core) and Pas des Sables (section S3; Fig. 8.4).

The most widespread lapilli bed of the Piton de la Fournaise's recent history is the "Black Tephra" unit, which marks the beginning of Chisny cone activity and is here dated for the first time at  $381 \pm 26$  BP (Er-14 Table 8.1). It likely represents the most explosive magmatic event of a series of eccentric eruptions that have occurred along the three rift zones (NW, SE and NE) in a short and recent period (1400–1600 CE; Er-10 to Er-18 Table 8.1; Tanguy et al. 2011). Interestingly, this series of closely spaced violent eruptions immediately preceded the first permanent human settlements on the island; consequently, without leaving any trace in the historical record.

---

## 5 Concluding Discussion

The characterization of the explosive activity and the research of violent paroxystic events over PdF massif has been performed through a drilling and excavation campaign supported by the integration of new radiocarbon ages to previous chronologic data. The use of a light shallow and continuous drilling system has proved to be a suitable methodology to execute surveys in an impervious territory, such in La Réunion, and to realize a detailed micro-stratigraphic study of the tephra emitted by the volcano over a relative recent period (last 5 kiloyear).

The stratigraphic study carried out on the cores confirms the presence of the "Bellecombe Ash unit" in a relatively superficial position, over a wide area ranging from the proximal area, near the Bellecombe caldera cliff and the Plaine des Sables, to at least the Plaine des Remparts, the middle-distal sector. The observation made at the microscopic scale does not allow us to extend this correlation to the most distal Grand Étang drill, located at 18 km from the PdF central cone, suggesting either the lacking of this deposit in the more distal areas or an age of the cones of Grand Étang younger than 3 kiloyear. Actually, the

uncertainty about the age of the pyroclastic cones which close the Grand Etang lake basin (younger than  $5730 \pm 110$  year BP; Banton 1985) does not permit to constrain its stratigraphic position with respect to Bellecombe ashes. Occurrence of "Bellecombe" layers (<20 cm total thickness) on the Trous Blancs area ca. 13 km W-NW from the central cone suggest that this is the main dispersion axis of these ashes.

The review of the Bellecombe Ash unit shows that only few ash fallout beds attain the medial area, with a thickness quickly decreasing when moving away from the Enclos Fouqué caldera. These decimeter-thick beds correspond to the upper part of the type-section described by Mohamed-Abchir (1996) in proximal areas. The age interval (3735–3060 BP) of the upper beds results significantly younger than that of the lower beds (4880–4175 BP) and of the lava flow underlying the ashes near the rim of the Enclos Fouqué caldera (4745 BP) (Bachelery 1981; Staudacher and Allègre 1993). The "Partage Tephra" sequence, here described for the first time, can thus represent a sequence of events marking the end of the "Bellecombe ash unit" and puts an upper limit for the Enclos Fouqué caldera collapse events (2340 year BP for Unit 2). Therefore the Bellecombe Ash unit groups a sequence of eruptive events, which span a much wider time-period than previously thought. Anyhow, it represents the most traceable horizon (Fig. 8.5) among the studied deposits and no other pyroclastic blanket exhibits a similar regional dispersion in the last 5 kiloyear.

A second, more limited, correlation has been found in the drilling cores. It involves the "Black Tephra" lapilli bed drilled in the Plaine des Sables (PDS1 and PDS2, Fig. 8.5). The "Black Tephra" originates and is mainly distributed westward (Fig. 8.4) within the Plaine des Sables from possibly linear (fracture) source structure. The deposit dispersal exhibits a W elongation, in agreement with the Easterlies direction at Pas de Bellecombe (inset in Fig. 8.4, ground level records by Météo France). Such fact highlights that an eventual plume generated during the eruption was confined below the Trade winds inversion zone, at about 4 km a.s.l., and thus cannot exceed the height of about 2 km

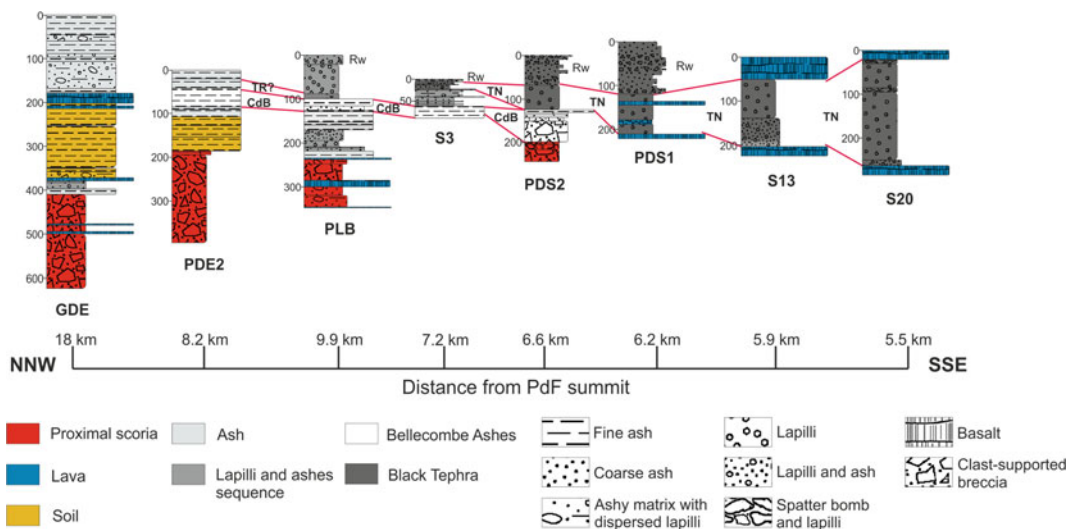


**Fig. 8.5** Stratigraphic correlations from the distal to the proximal sector at NW of Piton de la Fourmaise volcano. *CdB* Bellecombe Ashes; *TN* Black Tephra; *TR?* Red Tephra possible correlation; *Rw* reworked lapilli and ash

inasmuch the tephra source is located at an altitude of 2300 m a.s.l. The Black Tephra maximum dispersal seems to vanish quickly, within about 3.7 km in the downwind direction and over an area of less than 13 km<sup>2</sup>. This deposit presents the typical features of the hawaiian activity. In particular it seems to be related to a lava fountaining generated through a fissural source. This activity results to be very young ( $381 \pm 26$  BP); calibrated ages (1447–1628 CE) suggest this unusual event occurred shortly before the beginning of permanent settlement on La Réunion island.

A fountaining activity of similar intensity to that of the Chisny event is possibly represented by the Red Tephra unit dispersed in the medial area. This deposit could be represented in the PLB core (Plaine des Remparts West) upper black lapilli sequence at least by the basal red ash-coated lapilli (Table 8.4) and in the PDE2 core (Plaine des Remparts East) by the reddish ash layer overlying the Bellecombe Ash unit (Table 8.3). However this correlation still remains a hypothesis to verify cause of the scarce characterization for the middle-distal sector deposits. The age of this event (younger than 3200 BP) and its stratigraphic position suggests that it occurred near the end of the Bellecombe ash unit emplacement.

Besides the Bellecombe Ash unit, the lack of regionally distributed lapilli blankets suggests that no violent strombolian or more intense eruptions (subplinian to plinian) have occurred in the recent story of the volcano's activity (<5 kiloyear). In particular, the distribution of the “Partage Tephra” sequence highlights that phreatomagmatic events can impact the proximal areas outside the Enclos Fouqué caldera, but with a limited extension. Moreover, the lack of a continuous lapilli/ash horizon from the proximal to distal areas points out that the lapilli cover that overlay the Plaine des Sables and the Plaine des Remparts is the result of several local blankets linked to several hawaiian to strombolian emission centers. As highlighted by new radiocarbon ages obtained on tephra lying on the Langevin Plateau and Plaine des Sables (respectively 868, 620 and 381 year BP in Table 8.1) this kind of activity persisted in the N120° rift up to very recent times and ended probably just before the island's colonization, leaving no trace in historical records. The eccentric activity persisted instead along the NE and SE rift zones but with a dominantly effusive style (Michon et al. 2013).

The maximum expected magmatic events have therefore to be related to intense hawaiian fountaining. The Black Tephra unit, emitted by a



source area located near the Piton Chisny cone, represents a very recent and intense manifestation of this typology. The low amount of fine ashes and the NW elongation of its deposit, in fact, suggest the absence of the well-developed “cineritic” plume, which characterizes violent strombolian eruptions. Therefore, the implication for the risk assessment, and consequently for risk maps production and organization, must consider that lava fountaining, even if more vigorous than the normal, is the maximum magmatic explosive activity produced by Piton de la Fournaise in the last 5000 years. It implies that its dangerousness is restricted to a relatively brief distance from the source and that a regional deposition is strongly unlikely. The hazard represented by this type of activity resides in the possible positioning of the vent close to inhabited areas and in the possible occurrence of repeated events with short but unpredictable time interval from one to the other. Forecasting the location of the future eccentric eruptions is thus of paramount importance to minimize the potential impact of mild eruptions on the inhabitants and the structures.

**Acknowledgments** The Préfecture, Protection Civile and DEAL of the La Réunion and the MEEDDAT (Ministère de l’Ecologie, du Développement Durable et de l’Energie) are acknowledged for promoting, supporting and partially financing this project on volcanic hazard assessment at Piton de la Fournaise (convention n°11\_037 and 1321; 2011–2014). A. Morandi was supported by a grant of the Department of Earth Sciences of the University of Florence (entitled to prof. Orlando Vaselli).

## References

- Andronico D, Cristaldi A, Del Carlo P, Taddeucci J (2009) Shifting styles of basaltic explosive activity during the 2002–03 eruption of Mt. Etna. Italy. *J Volcanol Geotherm Res* 180:110–122
- Arrighi S, Principe C, Rosi M (2001) Violent strombolian and subplinian eruptions at Vesuvius during post-1631 activity. *Bull Volcanol* 63:126–150
- Bachèlery P (1981) Le Piton de la Fournaise (Ile de la Réunion). Etude Volcanologique, Structurale et Pétrologique. Thèse de l’Université de Clermont Ferrand, p. 217
- Banton O (1985) Rapport de thèse: Etude hydrogéologique d’un complexe alluvial en pays volcanique, sous climat tropical, site du Grand Étang—Ile de la Réunion. Université des sciences et techniques du Languedoc de Montpellier et Université française de l’Océan Indien, Atelier duplication—USTL, p 237
- Delorme H, Bachèlery P, Blum PA, Cheminée J-L, Delarue J, Delmond J, Hirn A, Lepine J, Vincent P, Zlotnicki J (1989) March 1986 eruptive episodes at Piton de la Fournaise volcano (Réunion Island). *J Volcanol Geotherm Res* 36:199–208
- Di Muro and project team (2012) Evaluation de l’alea volcanique a La Réunion. Rapport final-année I°. Projet BRGM/IPGP, p 80
- Fontaine FJ, Rabinowicz M, Boulègue Jouniaux L (2002) Constraints on hydrothermal processes on basaltic edifices: inferences on the conditions leading to hydrovolcanic eruptions at Piton de la Fournaise, Réunion Island, Indian Ocean. *Earth Planet Sci Lett* 200:1–14
- Fretzdorff S, Paterne M, Stoffers P, Ivanova E (2000) Explosive activity of the Reunion Island volcanoes through the past 260,000 years as recorded in deep-sea sediments. *Bull Volcanol*. doi:[10.1007/s004450000095](https://doi.org/10.1007/s004450000095)
- Houghton BF, Wilson CJN, Del Carlo P, Coltelli M, Sable JE, Carey RJ (2004) The influence of conduit processes on changes in style of basaltic Plinian eruptions: Tarawera 1886 and Etna 122 BC. *J Volcanol Geotherm Res* 137:1–14
- Hugoulin F (1860) Dernière éruption du volcan de l’île de la Réunion (19 mars 1860). *Revue algérienne et coloniale* 2:483–487
- Kieffer G, Tricot B, Vincent PM, (1977) Une éruption inhabituelle (Avril 1977) du Piton de La Fournaise (Ile de La Réunion): ses enseignements volcanologiques et structuraux. *C R Acad Sci Paris*, 285(D): 957–960
- Lesouëf D, Gheusi F, Delmas R, Escobar J (2011) Numerical simulations of local circulations and pollution transport over Reunion Island. *Ann Geophys* 29:53–69
- Lénat J-L (2016) A brief history of the observation of Piton de la Fournaise central area. In: Bachèlery P, Lénat J-F, Di Muro A, Michon L (eds) Active volcanoes of the Southwest Indian Ocean: Piton de la Fournaise and Karthala. Active Volcanoes of the World. Springer, Berlin
- Lénat JF, Bachèlery P (1988) Dynamics of magma transfer at Piton de la Fournaise volcano (Réunion Island, Indian Ocean). In: Chi-Yu et Scarpa (eds) Earth evolution sciences special issue “Modeling of Volcanic Processes”. Friedr. Vieweg and Sohn, Braunschweig/Wiesbaden, pp 57–72
- Lénat JF, Bachèlery P, Desmulier F (2001) Genèse du champ de lave de l’Enclos Fouqué: une éruption d’envergure exceptionnelle du Piton de la Fournaise (Réunion) au 18 ème siècle. *Bull Soc Géol Fr* 2:177–188
- Ludden JN (1977) Eruptive patterns for the volcano Piton de la Fournaise, Reunion Island. *J Volcanol Geotherm Res* 2:385–395
- Macdonald GA (1972) Volcanoes. Prentice-Hall inc., Englewood Cliffs, New Jersey. p 510



- Michon L, Di Muro A, Villeneuve N, Saint-Marc C, Fadda P, Manta F (2013) Explosive activity of the summit cone of Piton de la Fournaise volcano (La Réunion island): a historical and geological review. *J Volcanol Geotherm Res* 263:117–133
- Michon L, Ferrazzini V, Di Muro A (2016) Magma paths at Piton de la Fournaise volcano. In: Bachèlery P, Lénat J-F, Di Muro A, Michon L (eds) *Active volcanoes of the Southwest Indian Ocean: Piton de la Fournaise and Karthala. Active Volcanoes of the World*. Springer, Berlin
- Mohamed-Abchir MA (1996) *Les Cendres de Bellecombe: Un événement majeur dans le passé récent du Piton de la Fournaise*. Thèse d'université, Univ. de Paris VII, Paris, Ile de la Réunion
- Peltier A, Massin F, Bachèlery P, Finizola A (2012) Internal structures and building of basaltic shield volcanoes: the example of the Piton de La Fournaise terminal cone (La Réunion). *Bull Volcanol*. doi:10.1007/s00445-012-0636-7
- Pioli L, Erlund E, Johnson E, Cashman K, Wallace P, Rosi M, Delgado Granados H (2008) Explosive dynamics of violent strombolian eruptions: the eruption of Parícutin volcano 1943–1952 (Mexico). *Earth Planet Sci Lett* 271:359–368
- Principe C, Malfatti A, Rosi M, Ambrosio M, Fagioli MT (1997) Metodologia innovativa di carotaggio microstratigrafico: esempio di applicazione alla tefrostratigrafia di prodotti vulcanici distali. *Geol Tec Ambient* 4 (97):39–50
- Principe C, Malfatti A, Ambrosio M, Fagioli MT, Rosi M, Ceccanti B, Arrighi S, Innamorati D (2007) Finding distal Vesuvius tephra at the borders of Lago Grande di Monticchio. In: *AF shallow coring system micro-cores. Atti Soc Tosc Sci Nat Mem Serie A*, 112:189–197
- Roult G, Peltier A, Taisne B, Staudacher T, Ferrazzini V, Di Muro A, OVPF team (2012) A new comprehensive classification of the Piton de la Fournaise activity spanning the 1985–2010 period. Search and analysis of short-term precursors from a broad-band seismological station. *J Volcanol Geotherm Res* 241:78–104
- Sable JE, Houghton BF, Del Carlo P, Coltelli M (2006) Changing conditions of magma ascent and fragmentation during the Etna 122 BC basaltic Plinian eruption: evidence from clast microtextures. *J Volcanol Geotherm Res* 158:333–354
- Sable JE, Houghton BF, Wilson CJN, Carey R (2009) Eruption mechanisms during the climax of the Tarawera 1886 basaltic Plinian inferred from microtextural characteristics of deposits. In: Larsen G, Rowland SK, Self S, Hoskuldsson A (eds) *Thordarson T. Studies in Volcanology, The Legacy of George Walker*, pp 129–154
- Sisavath E, Mazuel A, Jorry SJ, Babonneau N, Bachèlery P, de Voogd B, Salpin M, Emmanuel L, Beaufort L, Toucanne S (2012) Processes controlling a volcaniclastic turbiditic system during the last climatic cycle: example of the Cilaos deep-sea fan, offshore La Réunion Island. *Sediment Geol* 281:180–193. doi:10.1016/j.sedgeo.2012.09.010
- Staudacher T, Allègre CJ (1993) Ages of the second caldera of Piton de la Fournaise volcano (Réunion) determined by cosmic ray produced  $^3\text{He}$  and  $^{21}\text{Ne}$ . *Earth Planet Sci Lett* 119:395–404
- Staudacher T, Peltier A, Ferrazzini V, Di Muro A, Boissier P, Catherine P, Kowalski P, Lauret F (2016) Fifteen years of intense (1998–2013) at Piton de La Fournaise volcano: a review. In: Bachèlery P, Lénat J-F, Di Muro A, Michon L (eds) *Active volcanoes of the Southwest Indian Ocean: Piton de la Fournaise and Karthala. Active Volcanoes of the World*. Springer, Berlin
- Stieltjes L, Moutou P (1989) A statistical and probabilistic study of the historic activity of the Piton de la Fournaise, Réunion Island, Indian Ocean. *J Volcanol Geotherm Res* 36:67–86
- Tanguy JC, Bachèlery P, Le Goff M (2011) Archeomagnetism of Piton de la Fournaise: bearing on volcanic activity at La Réunion Island and geomagnetic secular variation in Southern Indian Ocean. *Earth Planet Sci Lett* 303:361–368. doi:10.1016/j.epsl.2011.01.019
- Taupin FG, Bessafi M, Baldy S, Brémaud PJ (1999) Tropospheric ozone above the southwestern Indian Ocean is strongly linked to dynamical conditions prevailing in the tropics. *J Geophys Res* 104:8057–8066
- Tulet P, Villeneuve N (2011) Large scale modeling of the transport, chemical transformation and mass budget of the sulfur emitted during the eruption of April 2007 by the Piton de la Fournaise. *Atmos Chem Phys* 11:4533–4546
- Trenberth KE, Large WG, Olson JG (1990) The mean annual cycle in global ocean wind stress. *J Phys Oceanogr* 20:1742–1760
- Upton BGJ, Semet MP, Joron JL (2000) clasts in the, Piton de la Fournaise, Réunion Island, and their bearing on cumulative processes in the petrogenesis of the Réunion lavas. *J Volcanol Geotherm Res* 104:297–318
- Villeneuve N, Bachèlery P (2006) *Revue de la typologie des éruptions au Piton de La Fournaise, processus et risques volcaniques associés*. Cybergeo: revue européenne de Géographie, n° 336
- Wong LJ, Larsen JF (2010) The middle scoria sequence: a Holocene Subplinian and of Okmok volcano, Alaska. *Bull Volcanol* 72:17–31. doi:10.1007/s00445-009-0301-y